The Sloan Digital Sky Survey Quasar Catalog IV. Fifth Data Release

Donald P. Schneider,[1] Patrick B. Hall,[2] Gordon T. Richards,[3,4] Michael A. Strauss,[5] Daniel E. Vanden Berk,[1] Scott F. Anderson,[6] W.N. Brandt,[1] Xiaohui Fan,[7] Sebastian Jester,[8,9] Jim Gray,[10] James E. Gunn,[5] Mark U. SubbaRao,[11] Anirudda R. Thakar,[3] Chris Stoughton,[12] Alexander S. Szalay,[3] Brian Yanny,[12] Donald G. York,[13,14] Neta A. Bahcall,[5] J. Barentine,[15] Michael R. Blanton,[16] Howard Brewington,[15] J. Brinkmann,[15] Robert J. Brunner,[17] Francisco J. Castander,[18] István Csabai,[19] Joshua A. Frieman,[20,12,13] Masataka Fukugita,[21] Michael Harvanek,[15] David W. Hogg,[16] Željko Ivezić,[6] Stephen M. Kent,[12,13] S. J. Kleinman,[15] G.R. Knapp,[5] Richard G. Kron,[13,12] Jurek Krzesiński,[22] Daniel C. Long,[15] Robert H. Lupton,[5] Atsuko Nitta,[23] Jeffrey R. Pier,[24] David H. Saxe,[25] Yue Shen,[5] Stephanie A. Snedden,[15] David H. Weinberg,[26] and Jian Wu[1]

[1] Department of Astronomy and Astrophysics, The Pennsylvania State University, 525 Davey Laboratory, University Park, PA 16802.

[2] Department of Physics & Astronomy, York University, 4700 Keele Street, Toronto, Ontario, M3J 1P3, Canada.

[3] Department of Physics and Astronomy, The Johns Hopkins University, 3400 North Charles Street, Baltimore, MD 21218-2686.

[4] Department of Physics, Drexel University, 3141 Chestnut Street, Philadelphia, PA 19104.

[5] Princeton University Observatory, Peyton Hall, Princeton, NJ 08544.

[6] Department of Astronomy, University of Washington, Box 351580, Seattle, WA 98195.

[7] Steward Observatory, University of Arizona, 933 North Cherry Avenue, Tucson, AZ 85721.

[8] School of Physics and Astronomy, University of Southampton, Southampton SO17 1BJ, UK.

[9] Max-Planck-Institut für Astronomie, Königstuhl 17, D-69117 Heidelberg, Germany.

[10] Microsoft Research, 301 Howard Street, No. 830, San Francisco, CA 94105.

[11] University of Chicago and Adler Planetarium and Astronomy Museum, 1300 S. Lake Shore Drive, Chicago, IL 60605.

[12] Fermi National Accelerator Laboratory, P.O. Box 500, Batavia, IL 60510.

[13] Department of Astronomy and Astrophysics, The University of Chicago, 5640 South Ellis Avenue, Chicago, IL 60637.

[14] Enrico Fermi Institute, The University of Chicago, 5640 South Ellis Avenue, Chicago, IL 60637.

[15] Apache Point Observatory, P.O. Box 59, Sunspot, NM 88349.

[16] Department of Physics, New York University, 4 Washington Place, New York, NY 10003.

[17] Department of Astronomy, University of Illinois at Urbana-Champaign, 1002 West Green Street, Urbana, IL 61801-3080.

[18] Institut de Ciències de l'Espai (CSIC-IEEC), Campus UAB, 08193 Bellaterra, Barcelona, Spain.

[19] Department of Physics of Complex Systems, Eötvös University, Budapest, Pf. 32, H-1518 Budapest, Hungary.

[20] Center for Cosmological Physics, The University of Chicago, 5640 South Ellis Avenue Chicago, IL 60637.

[21] Institute for Cosmic Ray Research, University of Tokyo, 5-1-5 Kashiwa, Kashiwa City, Chiba 277-8582, Japan.

[22] Mt. Suhora Observatory, Cracow Pedagogical University, ul. Podchorazych 2, 30-084 Cracow, Poland.

[23] Gemini Observatory, 670 North A'ohoku Place, Hilo, HI 96720.

[24] US Naval Observatory, Flagstaff Station, P.O. Box 1149, Flagstaff, AZ 86002.

[25] 490 Wilson's Crossing Road, Auburn, NH 03032.

ABSTRACT

We present the fourth edition of the Sloan Digital Sky Survey (SDSS) Quasar Catalog. The catalog contains 77,429 objects; this is an increase of over 30,000 entries since the previous edition. The catalog consists of the objects in the SDSS Fifth Data Release that have luminosities larger than $M_i = -22.0$ (in a cosmology with $H_0 = 70$ km s^{-1} Mpc^{-1}, $\Omega_M = 0.3$, and $\Omega_\Lambda = 0.7$), have at least one emission line with FWHM larger than 1000 km s^{-1} or have interesting/complex absorption features, are fainter than $i \approx 15.0$, and have highly reliable redshifts. The area covered by the catalog is ≈ 5740 deg^2. The quasar redshifts range from 0.08 to 5.41, with a median value of 1.48; the catalog includes 891 quasars at redshifts greater than four, of which 36 are at redshifts greater than five. Approximately half of the catalog quasars have $i < 19$; nearly all have $i < 21$. For each object the catalog presents positions accurate to better than $0.2''$ rms per coordinate, five-band (*ugriz*) CCD-based photometry with typical accuracy of 0.03 mag, and information on the morphology and selection method. The catalog also contains basic radio, near-infrared, and X-ray emission properties of the quasars, when available, from other large-area surveys. The calibrated digital spectra cover the wavelength region 3800–9200 Å at a spectral resolution of $\simeq 2000$; the spectra can be retrieved from the public database using the information provided in the catalog. The average SDSS colors of quasars as a function of redshift, derived from the catalog entries, are presented in tabular form. Approximately 95% of the objects in the catalog were discovered by the SDSS.

Subject headings: catalogs, surveys, quasars:general

1. Introduction

This paper describes the Fourth Edition of the Sloan Digital Sky Survey (SDSS; York et al. 2000) Quasar Catalog. Previous versions of the catalog (Schneider et al. 2002, 2003, 2005; hereafter Papers I, II, and III) were published with the SDSS Early Data Release (EDR; Stoughton et al. 2002), the SDSS First Data Release (DR1; Abazajian et al. 2003), and the SDSS Third Data Release (DR3; Abazajian et al. 2005), and contained 3,814, 16,713, and

[26] Department of Astronomy, Ohio State University, 140 West 18th Avenue, Columbus, OH 43210-1173.

46,420 quasars, respectively. The current catalog is the entire set of quasars from the SDSS-I Quasar Survey; the SDSS-I was completed on 30 June 2005 and the Fifth Data Release (DR5; Adelman-McCarthy et al. 2007) was made public on 30 June 2006. The catalog contains 77,429 quasars, the vast majority of which were discovered by the SDSS. The SDSS Quasar Survey is continuing via the SDSS-II Legacy Survey, which is is an extension of the SDSS-I.

The catalog in the present paper consists of the DR5 objects that have a luminosity larger than $M_i = -22.0$ (calculated assuming an $H_0 = 70$ km s^{-1} Mpc^{-1}, $\Omega_M = 0.3$, $\Omega_\Lambda = 0.7$ cosmology [Spergel et al. 2006], which will be used throughout this paper), and whose SDSS spectra contain at least one broad emission line (velocity FWHM larger than ≈ 1000 km s^{-1}) or have interesting/complex absorption-line features. The catalog also has a bright limit of $i \approx 15.0$. The quasars range in redshift from 0.08 to 5.41; 78% have redshifts below 2.0.

The objects are denoted in the catalog by their DR5 J2000 coordinates; the format for the object name is SDSS Jhhmmss.ss+ddmmss.s. Since the image data used for the astrometric information can change between data releases (e.g., a region with poor seeing that is included in an early release is superseded by a newer observation in good seeing), the coordinates for an object can change at the $0.1''$ to $0.2''$ level; hence the designation of a given source can change between data releases. Except on very rare occasions (see §5.1), this change in position is much less than $1''$. When merging SDSS Quasar Catalogs with previous databases one should always use the coordinates, not object names, to identify unique entries.

The DR5 catalog does not include classes of Active Galactic Nuclei (AGN) such as Type 2 quasars, Seyfert galaxies, and BL Lacertae objects; studies of these sources in the SDSS can be found in Zakamska et al. (2003) (Type 2), Kauffmann et al. (2003) and Hao et al. (2005) (Seyferts), and Collinge et al. (2005) and Anderson et al. (2007) (BL Lacs). Spectra of the highest redshift SDSS quasars ($z > 5.7$; e.g., Fan et al. 2003, 2006a) were not acquired as part of the SDSS quasar survey (the objects were identified as candidates in the SDSS imaging data, but the spectra were not obtained with the SDSS spectrographs), so they are not included in the catalog.

The observations used to produce the catalog are presented in Section 2; the construction of the catalog and the catalog format are discussed in Sections 3 and 4, respectively. Section 5 presents an overview of the catalog, and a summary is given in Section 6. The catalog is presented in an electronic table in this paper and can also be found at an SDSS public web site.[1]

[1] `http://www.sdss.org/dr5/products/value_added/qsocat_dr5.html`

2. Observations

2.1. Sloan Digital Sky Survey

The Sloan Digital Sky Survey uses a CCD camera (Gunn et al. 1998) on a dedicated 2.5-m telescope (Gunn et al. 2006) at Apache Point Observatory, New Mexico, to obtain images in five broad optical bands (*ugriz*; Fukugita et al. 1996) over approximately 10,000 deg^2 of the high Galactic latitude sky. The survey data-processing software measures the properties of each detected object in the imaging data in all five bands, and determines and applies both astrometric and photometric calibrations (Pier et al., 2003; Lupton et al. 2001; Ivezić et al. 2004). Photometric calibration is provided by simultaneous observations with a 20-inch telescope at the same site (see Hogg et al. 2001, Smith et al. 2002, Stoughton et al. 2002, and Tucker et al. 2006). The SDSS photometric system is based on the AB magnitude scale (Oke & Gunn 1983).

The catalog contains photometry from 204 SDSS imaging runs acquired between 19 September 1998 (Run 94) and 1 June 2005 (Run 5326).

2.2. Target Selection

The SDSS filter system was designed to identify quasars at redshifts between zero and approximately six; most quasar candidates are selected based on their location in multidimensional SDSS color-space. The Point Spread Function (PSF) magnitudes are used for the quasar target selection, and the selection is based on magnitudes and colors that have been corrected for Galactic extinction (using the maps of Schlegel, Finkbeiner, & Davis 1998). An i magnitude limit of 19.1 is imposed for candidates whose colors indicate a probable redshift of less than ≈ 3.0 (selected from the *ugri* color cube); high-redshift candidates (selected from the *griz* color cube) are accepted if $i < 20.2$ and the source is unresolved. The errors on the i measurements are typically 0.02–0.03 and 0.03–0.04 magnitudes at the brighter and fainter limits, respectively. In addition to the multicolor selection, unresolved objects brighter than $i = 19.1$ that lie within $2.0''$ of a FIRST radio source (Becker, White, & Helfand 1995) are also identified as primary quasar candidates. Target selection also imposes a maximum brightness limit ($i \approx 15.0$) on quasar candidates; the spectra of objects that exceed this brightness could contaminate the adjacent spectra on the detectors of the SDSS spectrographs. A detailed description of the quasar selection process and possible biases can be found in Richards et al. (2002a).

The primary sample described above was supplemented by quasars that were targeted

by the following SDSS spectroscopic target selection algorithms: Galaxy and Luminous Red Galaxy (Strauss et al. 2002 and Eisenstein et al. 2001), X-ray (object near the position of a *ROSAT* All-Sky Survey [RASS; Voges et al. 1999, 2000] source; see Anderson et al. 2003), Star (point source with a color typical of an interesting class of star), or Serendipity (unusual color or FIRST matches). The SDSS is designed to be complete in the Galaxy, Luminous Red Galaxy and Quasar programs, (in practice various limitations reduce the completeness to about 90%) but no attempt at completeness was made for the last three categories. Most of the DR5 quasars that fall below the magnitude limits of the quasar survey were selected by the serendipity algorithm (see §5).

While the bulk of the catalog objects targeted as quasars were selected based on the algorithm of Richards et al. (2002a), during the early years of the SDSS the quasar selection software was undergoing constant modification to improve its efficiency. All of the sources in Papers I and II, and some of the Paper III objects, were not identified with the final selection algorithm. Once the final target selection software was installed, the algorithm was applied to the entire SDSS photometric database. Each DR5 quasar has two spectroscopic target selection flags listed in the catalog: BEST, which refers to the final algorithm, and TARGET, which is the target flag used in the actual spectroscopic targeting. There are also two sets of photometric measurements for each quasar: BEST, which refers to the measurements with the latest photometric software on the highest quality data, and TARGET, which are the values used at the time of the spectroscopic target selection.

Extreme care must be exercised when constructing statistical samples from this catalog; if one uses the values produced by only the latest version of the selection software, not only must one drop the catalog quasars that were not identified as quasar candidates by the final selection software, one must also account for quasar candidates produced by the final version that were not observed in the SDSS spectroscopic survey (this can occur in regions of sky whose spectroscopic targets were identified by early versions of the selection software). The selection for the UV-excess quasars, which comprise the majority ($\approx 80\%$) of the objects in the DR5 Catalog, has remained reasonably uniform; the changes to the selection algorithm were primarily designed to increase the effectiveness of the identification of $3.0 < z < 3.8$ quasars. Extensive discussion of the completeness and efficiency of the selection can be found in Richards et al. (2002a) and Vanden Berk et al. (2005); Richards et al. (2006) describes the process for the construction of statistical SDSS quasar samples (see also Adelman-McCarthy et al. 2007). The survey efficiency (the ratio of quasars to quasar candidates) for the ultraviolet excess-selected candidates, which comprise the bulk of the quasar sample, is about 77%. (The catalog contains information on which objects can be used in a uniform sample; see Section 4.)

2.3. Spectroscopy

Spectroscopic targets chosen by the various SDSS selection algorithms (i.e., quasars, galaxies, stars, serendipity) are arranged onto a series of 3° diameter circular fields (Blanton et al. 2003). Details of the spectroscopic observations can be found in York et al. (2000), Castander et al. (2001), Stoughton et al. (2002), and Paper I. A total of 1458 spectroscopic fields, taken between 5 March 2000 and 14 June 2005, provided the quasars for the DR5 quasar catalog; the locations of the plate centers can be found from the information given by Adelman-McCarthy et al. (2007). The DR5 spectroscopic program attempted to cover, in a well-defined manner, an area of ≈ 5740 deg^2. Spectroscopic plate 716 was the first spectroscopic observation that was based on the final version of the quasar target selection algorithm of Richards et al. (2002a); the detailed tiling information in the SDSS database must be consulted to identify those regions of sky targeted with the final selection algorithm (see Richards et al. 2006).

The two SDSS double spectrographs produce data covering 3800–9200 Å at a spectral resolution of $\simeq 2000$. The data, along with the associated calibration frames, are processed by the SDSS spectroscopic pipeline (see Stoughton et al. 2002). The calibrated spectra are classified into various groups (e.g., star, galaxy, quasar), and redshifts are determined by two independent software packages. Objects whose spectra cannot be classified by the software are flagged for visual inspection. Figure 1 shows the calibrated SDSS spectra of four previously unknown catalog quasars representing a range of properties. The processed DR5 spectra *have not* been corrected for Galactic extinction.

3. Construction of the SDSS DR5 Quasar Catalog

The quasars in the catalog were drawn from three sets of SDSS observations: 1) the primary survey area, 2) "Bonus" plates, which are spectroscopic observations of regions near to, but outside of, the primary survey area, and 3) "Special" plates, where the spectroscopic targets were not chosen by the standard SDSS target selection algorithms (e.g., a set of plates to investigate the structure of the Galaxy; see Adelman-McCarthy et al. 2006).

The DR5 quasar catalog was constructed, as were the previous editions, in three stages: 1) Creation of a quasar candidate database, 2) Visual examination of the spectra of the quasar candidates, and 3) Application of luminosity and emission-line velocity width criteria. All three tasks were initially done without reference to the material in the previous SDSS Quasar Catalogs, although the results of each task were compared to the Paper III database (e.g., the construction of the quasar database was not viewed as complete until it was understood

why any Paper III quasars were not included).

3.1. Creation of the DR5 Quasar Candidate Database

This catalog of bona-fide quasars, that have redshifts checked by eye and luminosities and line widths that meet the formal quasar definition, is constructed from a larger "master" table of confirmed quasars and quasar candidates. This master table was created using an SQL query to the public SDSS-DR5 database (i.e., the Catalog Archive Server [CAS]; http://cas.sdss.org/astrodr5/). Two versions of the photometric database exist, which contain the properties of objects when targeted for spectroscopic observations (TARGET) and as determined in the latest processing (BEST). These databases are divided into multiple tables and subtables to facilitate access to only the most relevant data for a particular use. In the case of the quasar catalog construction, we have made use of the `PhotoObjAll` and `SpecObjAll` tables, which contain, respectively, the photometric information for *all* SDSS sources and for *all* SDSS spectra. In the case of `PhotoObjAll`, both the TARGET and BEST versions are queried. These tables include duplicate observations of objects and observations of objects that lie outside of the formal SDSS area (as compared to the `PhotoObj` and `SpecObj` tables, which include only sources in the formal SDSS area), and are the most complete database files. For example, in `PhotoObjAll`, two (or more) observations of a single object may exist; if so, one is classified as `PRIMARY`, the other(s) as `SECONDARY`.

This master table contains all objects identified as quasar candidate targets for spectroscopy in either the TARGET or BEST photometric databases. Quasar candidates are those objects which have had one or more of the following flags set by the algorithm described by Richards et al. (2002a):

```
TARGET_QSO_HIZ OR TARGET_QSO_CAP OR TARGET_QSO_SKIRT OR TARGET_QSO_FIRST_CAP
OR TARGET_QSO_FIRST_SKIRT
```

(= 0x0000001F, except for the "special" plates [see Adelman-McCarthy et al. 2006, 2007], where additional care is required in interpreting the flags).

Objects flagged as `TARGET_QSO_MAG_OUTLIER` and `TARGET_QSO_REJECT` are not included, as these flags are meant only for diagnostic purposes. (In the CAS documentation and the EDR paper, `TARGET_QSO_MAG_OUTLIER` is called `TARGET_QSO_FAINT`.) Furthermore, the master table includes any objects with spectra that have been classified by the spectroscopic pipeline as quasars (`specClass=QSO` or `HIZ_QSO`), that have `UNKNOWN` type, or that have redshifts greater than 0.6. (On rare occasions the spectroscopic pipeline measures the correct redshift for a quasar but classifies the object as a galaxy.)

The query was run on the union of the database tables `Target..PhotoObjAll`, `Best..SpecObjAll`, and `Best..PhotoObjAll`. Multiple entries for a given object are retained at this stage.

Ten objects in the DR3 Quasar Catalog were missed by this query. One omission was due to an "unmapped" fiber (a spectrum of a quasar was obtained, but because of a failure in the mapping of fiber number to location in the sky, we are no longer certain of the celestial position of the object); the other nine were low-redshift AGN that were not classified as quasars by the spectroscopic pipeline (this result provides an estimate of the incompleteness produced by the query). We were able to identify the information for all ten quasars in the database and add the material to the master table.

Four automated cuts were made to the master table database of 329,884 candidates [2]: 1) Objects targeted as quasars but whose spectra had not yet been obtained by the closing date of DR5 (124,447 objects), 2) Candidates classified with high confidence as "stars" by the spectroscopic pipeline that had redshifts less than 0.002 (33,653), 3) Objects whose photometric measurements have not been loaded into the CAS (3106) and 4) Multiple spectra (coordinate agreement better than $1.0''$) of the same object (40,007). In cases of duplicate spectra of an object, the "science primary" spectrum is selected (i.e., the spectrum was obtained as part of normal science operations); when there is more than one science primary observation (or when none of the spectra have this flag set), the spectrum with the highest signal-to-noise ratio (S/N) is retained (see Stoughton et al. 2002 for a description of the science primary flag). These actions produced a list of 128,671 unique quasar candidates.

3.2. Visual Examination of the Spectra

The SDSS spectra of the remaining quasar candidates were manually inspected by several of the authors (DPS, PBH, GTR, MAS, and SFA); as in previous papers in this series, we found that the spectroscopic pipeline redshifts and classifications of the overwhelming majority of the objects are accurate. Tens of thousands of objects were dropped from the list because they were obviously not quasars (these objects tended to be low S/N stars, unusual stars, and a mix of absorption-line and narrow emission-line objects); this large number of candidates that are not quasars is due to the inclusive nature of our initial database query. Spectra for which redshifts could not be determined (low signal-to-noise ratio or subject to data-processing difficulties) were also removed from the sample. This visual inspection resulted in the revisions of the redshifts of 863 quasars; the changes in the individual redshifts

[2]The master table is known as the QSOConcordanceALL table, which can be found in the SDSS database; see `http://cas.sdss.org/astrodr5/en/help/browser/description.asp?n=QsoConcordanceAll&t=U`.

were usually quite substantial, due to the spectroscopic pipeline misidentifying emission lines.

An independent determination of the redshifts of 5,865 quasars with redshifts larger than 2.9 in the catalog was performed by Shen et al. (2007). The redshift differences between the two sets of measurements follow a Gaussian distribution (with slightly extended wings), with a mean of 0.002 and a dispersion of 0.01.

The catalog contains numerous examples of extreme Broad Absorption Line (BAL) Quasars (see Hall et al. 2002); it is difficult if not impossible to apply the emission-line width criterion for these objects, but they are clearly of interest, have more in common with "typical" quasars than with narrow-emission line galaxies, and have historically been included in quasar catalogs. We have included in the catalog all objects with broad absorption-line spectra that meet the $M_i < -22.0$ luminosity criterion.

3.3. Luminosity and Line Width Criteria

As in Papers II and III, we adopt a luminosity limit of $M_i = -22.0$. The absolute magnitudes were calculated by correcting the BEST i measurement for Galactic extinction (using the maps of Schlegel, Finkbeiner, & Davis 1998) and assuming that the quasar spectral energy distribution in the ultraviolet-optical can be represented by a power law ($f_\nu \propto \nu^\alpha$), where $\alpha = -0.5$ (Vanden Berk et al. 2001). (In the 134 cases where BEST photometry was not available, the TARGET measurements were substituted for the absolute magnitude calculation.) This approach ignores the contributions of emission lines and the observed distribution in continuum slopes. Emission lines can contribute several tenths of a magnitude to the k-correction (see Richards et al. 2006), and variations in the continuum slopes can introduce a magnitude or more of error into the calculation of the absolute magnitude, depending upon the redshift. The absolute magnitudes will be particularly uncertain at redshifts near and above five, when the Lyman α emission line (with a typical observed equivalent width of $\approx 400 - 500$ Å) and strong Lyman α forest absorption enter the i bandpass.

Quasars near the $M_i = -22.0$ luminosity limit are often not enormously brighter in the i-band than the starlight produced by the host galaxy. Although the PSF-based SDSS photometry presented in the catalog are less susceptible to host galaxy contamination than are fixed-aperture measurements, the nucleus of the host galaxy can still contribute appreciably to this measurement for the lowest luminosity entries in the catalog (see Hao et al. 2005). An object of $M_i = -22.0$ will reach the $i = 19.1$ "low-redshift" selection limit at a redshift of ≈ 0.4.

After visual inspection and application of the luminosity criterion had reduced the

number of quasar candidates to under 80,000 objects, the remaining spectra were processed with an automated line-measuring routine. The spectra for objects whose maximum line width was less than 1000 km s^{-1} were visually examined; if the measurement was deemed to be an accurate reflection of the line (automated routines occasionally have spectacular failures when dealing with complex line profiles), the object was removed from the catalog.

4. Catalog Format

The DR5 SDSS Quasar Catalog is available in three types of files at the SDSS public web site listed in the introduction: 1) a standard ASCII file with fixed-size columns, 2) a gzipped compressed version of the ASCII file (which is smaller than the uncompressed version by a factor of nearly five), and 3) a binary FITS table format. The following description applies to the standard ASCII file. All files contain the same number of columns, but the storage of the numbers differs slightly in the ASCII and FITS formats; the FITS header contains all of the required documentation. Table 1 provides a summary of the information contained in each of the columns in the ASCII catalog.

The standard ASCII catalog (Table 2 of this paper) contains information on 77,429 quasars in a 36 MB file. The DR5 format is similar to that of DR3 with a few minor differences.

The first 80 lines consist of catalog documentation; this is followed by 77,429 lines containing information on the quasars. There are 74 columns in each line; a summary of the information is given in Table 1 (the documentation in the ASCII catalog header is essentially an expansion of Table 1). At least one space separates all the column entries, and, except for the first and last columns (SDSS designation and the object name if previously known), all entries are reported in either floating point or integer format.

Notes on the catalog columns:

1) The DR5 object designation, given by the format SDSS Jhhmmss.ss+ddmmss.s; only the final 18 characters are listed in the catalog (i.e., the "SDSS J" for each entry is dropped). The coordinates in the object name follow IAU convention and are truncated, not rounded.

2–3) The J2000 coordinates (Right Ascension and Declination) in decimal degrees. The positions for the vast majority of the objects are accurate to $0.1''$ rms or better in each coordinate; the largest expected errors are $0.2''$ (see Pier et al 2003). The SDSS coordinates are placed in the International Celestial Reference System, primarily through the United States Naval Observatory CCD Astrograph Catalog (Zacharias et al. 2000), and have an rms

accuracy of 0.045″ per coordinate.

4) The quasar redshifts. A total of 862 of the CAS redshifts were revised during our visual inspection. A detailed description of the redshift measurements is given in Section 4.10 of Stoughton et al. (2002). A comparison of 299 quasars observed at multiple epochs by the SDSS (Wilhite et al. 2005) found an rms difference of 0.006 in the measured redshifts for a given object. It is well known that the redshifts of individual broad emission lines in quasars exhibit significant offsets from their systemic redshifts (e.g., Gaskell 1982, Richards et al. 2002b, Shen et al. 2007); the catalog redshifts attempt to correct for this effect in the ensemble average (see Stoughton et al. 2002).

5–14) The DR5 PSF magnitudes and errors (not corrected for Galactic extinction) from BEST photometry for each object in the five SDSS filters. Some of the relevant imaging scans, such as special scans through M31 (see the DR4 and DR5 papers) were never loaded into the CAS, therefore the BEST photometry is not available for them. Thus there are 134 quasars which have entries of "0.000" for their BEST photometric measurements.

The effective wavelengths of the u, g, r, i, and z bandpasses are 3541, 4653, 6147, 7461, and 8904 Å, respectively (for an $\alpha = -0.5$ power-law spectral energy distribution using the definition of effective wavelength given in Schneider, Gunn, & Hoessel 1983). The photometric measurements are reported in the natural system of the SDSS camera, and the magnitudes are normalized to the AB system (Oke & Gunn 1983). The measurements are reported as asinh magnitudes (Lupton, Gunn, & Szalay 1999); see Adelman-McCarthy et al. (2007) for additional discussion and references for the accuracy of the photometric measurements. The TARGET PSF photometric measurements are presented in columns 63–72.

15) The Galactic extinction in the u band based on the maps of Schlegel, Finkbeiner, & Davis (1998). For an $R_V = 3.1$ absorbing medium, the extinctions in the SDSS bands can be expressed as

$$A_x \;=\; C_x \; E(B-V)$$

where x is the filter ($ugriz$), and values of C_x are 5.155, 3.793, 2.751, 2.086, and 1.479 for $ugriz$, respectively (A_g, A_r, A_i, and A_z are 0.736, 0.534, 0.405, and 0.287 times A_u).

16) The logarithm of the Galactic neutral hydrogen column density along the line of sight to the quasar. These values were estimated via interpolation of the 21-cm data from Stark et al. (1992), using the COLDEN software provided by the *Chandra* X-ray Center. Errors associated with the interpolation are typically expected to be less than $\approx 1 \times 10^{20}$ cm^{-2} (e.g., see §5 of Elvis, Lockman, & Fassnacht 1994).

17) Radio properties. If there is a source in the FIRST catalog within 2.0″ of the quasar position, this column contains the FIRST peak flux density at 20 cm encoded as an AB magnitude

$$AB \;=\; -2.5 \log \left(\frac{f_\nu}{3631 \text{ Jy}} \right)$$

(see Ivezić et al. 2002). An entry of "0.000" indicates no match to a FIRST source; an entry of "−1.000" indicates that the object does not lie in the region covered by the final catalog of the FIRST survey. The catalog contains 6226 FIRST matches; 5729 DR5 quasars lie outside of the FIRST area.

18) The S/N of the FIRST source whose flux is given in column 17.

19) Separation between the SDSS and FIRST coordinates (in arc seconds).

20) In cases when the FIRST counterpart to an SDSS source is extended, the FIRST catalog position of the source may differ by more than 2″ from the optical position. A "1" in column 20 indicates that no matching FIRST source was found within 2″ of the optical position, but that there *is* significant detection (larger than 3σ) of FIRST flux at the optical position. This is the case for 2440 SDSS quasars.

21) A "1" in column 21 identifies the 1596 sources with a FIRST match in either columns 17 or 20 that also have at least one FIRST counterpart located between 2.0″ (the SDSS-FIRST matching radius) and 30″ of the optical position. Based on the average FIRST source surface density of 90 deg^{-2}, we expect 50–60 of these matches to be chance superpositions.

22) The logarithm of the vignetting-corrected count rate (photons s^{-1}) in the broad energy band (0.1–2.4 keV) in the *ROSAT* All-Sky Survey Faint Source Catalog (Voges et al. 2000) and the *ROSAT* All-Sky Survey Bright Source Catalog (Voges et al. 1999). The matching radius was set to 30″; an entry of "−9.000" in this column indicates no X-ray detection. There are 4133 RASS matches in the DR5 catalog.

23) The S/N of the *ROSAT* measurement.

24) Separation between the SDSS and *ROSAT* All-Sky Survey coordinates (in arc seconds).

25–30) The JHK magnitudes and errors from the Two Micron All Sky Survey (2MASS; Skrutskie et al. 2006) All-Sky Data Release Point Source Catalog (Cutri et al. 2003) using a matching radius of 2.0″. A non-detection by 2MASS is indicated by a "0.000" in these columns. Note that the 2MASS measurements are Vega-based, not AB, magnitudes. The catalog contains 9824 2MASS matches.

31) Separation between the SDSS and 2MASS coordinates (in arc seconds).

32) The absolute magnitude in the i band calculated by correcting for Galactic extinction and assuming $H_0 = 70$ km s^{-1} Mpc^{-1}, $\Omega_M = 0.3$, $\Omega_\Lambda = 0.7$, and a power-law (frequency) continuum index of -0.5.

33) The $\Delta(g-i)$ color, which is the difference in the Galactic extinction corrected $(g-i)$ for the quasar and that of the mean of the quasars at that redshift. If $\Delta(g-i)$ is not defined for the quasar, which occurs for objects at either $z < 0.12$ or $z > 5.12$ the column will contain "−9.000". See Section 5.2 for a description of this quantity.

34) Morphological information. If the SDSS photometric pipeline classified the image of the quasar as a point source, the catalog entry is 0; if the quasar is extended, the catalog entry is 1.

35) The SDSS `SCIENCEPRIMARY` flag, which indicates whether the spectrum was taken as a normal science spectrum (`SCIENCEPRIMARY` = 1) or for another purpose (`SCIENCEPRIMARY` = 0). The latter category contains Quality Assurance and calibration spectra, or spectra of objects located outside of the nominal survey area. Over 90% of the DR5 entries (69,762 objects) are `SCIENCEPRIMARY` = 1.

36) This flag provides information on whether the photometric object is designated `PRIMARY` (1), `SECONDARY` (2), or `FAMILY` (3; these are blended objects that have not been deblended). During target selection, only `PRIMARY` objects are considered (except on occasion for objects located in fields that are not part of the nominal survey area); however, differences between TARGET and BEST photometric pipeline versions make it possible that the BEST photometric object belonging to a spectrum is either not detected at all, or is a non-primary object (see §3.1 above). Over 99% of the catalog entries are `PRIMARY`; 613 quasars are `SECONDARY` and 9 are `FAMILY`. There are 124 quasars with an entry of "0" in this column; each of these is an object that lacks BEST photometry. For statistical analysis, one should use only `PRIMARY` objects; `SECONDARY` and `FAMILY` objects are included in the catalog for the sake of completeness with respect to confirmed quasars.

37) The "uniform selection" flag, either 0 or 1; a "0" indicates that the object was not identified as a primary quasar target (39,855 catalog entries) with the final target selection algorithm.

38) The 32-bit SDSS target-selection flag from BEST processing (`PRIMTARGET`; see Table 26 in Stoughton et al. 2002 for details); this is the flag produced by running the selection algorithm of Richards et al. (2002a) on the most recent processing of the image data. The target-selection flag from TARGET processing is found in column 53.

39–45) The spectroscopic target selection breakdown (BEST) for each object. The target selection flag in column 38 is decoded for seven groups: Low-redshift quasar, High-redshift quasar, FIRST, ROSAT, Serendipity, Star, and Galaxy An entry of "1" indicates that the object satisfied the given criterion (see Stoughton et al. 2002). Note that an object can be, and often is, targeted by more than one selection algorithm. The last two columns in Table 3 presents the number of quasars identified by the individual BEST target selection algorithm; the column labeled "Sole" indicates the number of objects that were detected by only one of the seven listed selection algorithms.

46–47) The SDSS Imaging Run number and the Modified Julian Date (MJD) of the photometric observation used in the catalog. The MJD is given as an integer; all observations on a given night have the same integer MJD (and, because of the observatory's location, the same UT date). For example, imaging run 94 has an MJD of 51075; this observation was taken on 1998 September 19 (UT).

48–50) Information about the spectroscopic observation (Modified Julian Date, spectroscopic plate number, and spectroscopic fiber number) used to determine the redshift. These three numbers are unique for each spectrum, and can be used to retrieve the digital spectra from the public SDSS database.

51–54) Additional SDSS processing information: the photometric processing rerun number; the camera column (1–6) containing the image of the object, the field number of the run containing the object, and the object identification number (see Stoughton et al. 2002 for descriptions of these parameters).

55) The 32-bit SDSS target selection flag from the TARGET processing, i.e., the value that was used when the spectroscopic plate was drilled. This may not match the BEST target selection flag because a different versions of the selection algorithm were used, the selection was done with different image data (superior quality data of the field was obtained after the spectroscopic observations were completed), or different processings of the same data were used. Objects with no TARGET flag were either identified as quasars as a result of Quality Assurance observations and/or from special plates with somewhat different targeting criteria (see Adelman-McCarthy 2006).

56–62) The spectroscopic target-selection breakdown (TARGET) for each object; this is the same convention as followed in columns 39–45 for the BEST target-selection flag.

63–72) The DR5 PSF magnitudes and errors (not corrected for Galactic reddening) from TARGET photometry.

73) The 64-bit integer that uniquely describes the spectroscopic observation that is listed in

the catalog (SpecObjID).

74) Name of object in the NASA/IPAC Extragalactic Database (NED). If there is a source in the NED quasar database within 5.0″ of the quasar position, the NED object name is given in this column. The NED quasar database contains over 100,000 objects. Occasionally NED will list the SDSS name for objects that were not discovered by the SDSS.

5. Catalog Summary

The 77,429 objects in the catalog represent an increase of 31,009 quasars over the Paper III database; of the entries in the new catalog, 74,297 (96.0%) were discovered by the SDSS (with the caveat that NED is not complete). The catalog quasars span a wide range of properties: redshifts from 0.078 to 5.414, $14.94 < i < 22.36$ (506 objects have $i > 20.5$; only 26 have $i > 21.0$), and $-30.27 < M_i < -22.00$. The catalog contains 6226, 4133, and 9824 matches to the FIRST, RASS, and 2MASS catalogs, respectively. The RASS and 2MASS catalogs cover essentially all of the DR5 area, but 5729 (7%) of the entries in the DR5 catalog lie outside of the FIRST region.

Figure 2 displays the distribution of the DR5 quasars in the i-redshift plane (the 26 objects with $i > 21$ are not plotted). Objects which NED indicates were previously discovered by investigations other than the SDSS are indicated with open circles. The curved cutoff on the left hand side of the graph is produced by the minimum luminosity criterion ($M_i < -22.0$). The ridge in the contours at $i \approx 19.1$ for redshifts below three reflects the flux limit of the low-redshift sample; essentially all of the large number of $z < 3$ points with $i > 19.1$ are quasars selected via criteria other than the primary multicolor sample.

A histogram of the catalog redshifts is shown in the upper curve in Figure 3. A clear majority of quasars have redshifts below two (the median redshift is 1.48, the mode is ≈ 1.85), but there is a significant tail of objects extending out to redshifts beyond five ($z_{\rm max} = 5.41$). The dips in the curve at redshifts of 2.7 and 3.5 arise because the SDSS colors of quasars at these redshifts are similar to the colors of stars; we decided to accept significant incompleteness at these redshifts rather than be overwhelmed by a large number of stellar contaminants in the spectroscopic survey. Improvements in the quasar target selection algorithm since the initial editions of the SDSS Quasar Catalog have increased the efficiency of target selection at redshifts near 3.5 (compare Figure 3 with Paper II's Figure 4; see Richards et al. 2002a for a discussion of the incompleteness of the SDSS Quasar Survey).

This structure in the catalog redshift histogram can be understood by careful modelling of the selection effects (e.g., accounting for emission line effects and using only objects

selected in regions whose spectroscopic observations were chosen with the final version of the quasar target selection algorithm; also see Figure 8 in Richards et al. 2006). Repeating the analysis of Richards et al. (2006) for the DR5 sample reveals no structure in the redshift distribution after selection effects have been included (see lower histogram in Figure 3); this is in contrast to the reported redshift structure found in the SDSS quasar survey by Bell & McDiarmid (2006). To construct the lower histogram we have partially removed the effect of host galaxy contamination (by excluding extended objects), limited the sample to a uniform magnitude limit of $i < 19.1$ (accounting for emission-line effects), and have corrected for the known incompleteness near $z \sim 2.7$ and $z \sim 3.5$ due to quasar colors lying close to or in the stellar locus. Accounting for selection effects significantly reduces the number of objects as compared with the raw, more heterogeneous catalog, but the smaller, more homogeneous sample is what should be used for statistical analyses.

The distribution of the observed i magnitude (not corrected for Galactic extinction) of the quasars is given in Figure 4. The sharp drops in the histogram at $i \approx 19.1$ and $i \approx 20.2$ are due to the magnitude limits in the low and high-redshift samples, respectively.

Figures 5 and 6 display the distribution of the absolute i magnitudes of the catalog quasars. There is a roughly symmetric peak centered at $M_i = -26$ with a FWHM of approximately one magnitude. The histogram declines sharply at high luminosities (only 1.5% of the objects have $M_i < -28.0$) and has a gradual decline toward lower luminosities, partially due to host-galaxy contribution.

A summary of the spectroscopic selection, for both the TARGET and the BEST algorithms, is given in Table 3. We report seven selection classes in the catalog (columns 39 to 45 for BEST, 56–62 for TARGET). Each selection version has two columns, the number of objects that satisfied a given selection criterion and the number of objects that were identified only by that selection class. About two-thirds of the catalog entries were selected based on the SDSS quasar selection criteria (either a low-redshift or high-redshift candidate, or both). Slightly more than half of the quasars in the catalog are serendipity-flagged candidates, which is also primarily an "unusual color" algorithm; about one-fifth of the catalog was selected by the serendipity criteria alone.

Of the 50,093 DR5 quasars that have Galactic-absorption corrected TARGET i magnitudes brighter than 19.1, 48,593 (97.0%) were identified by the TARGET quasar multicolor selection; if one combines TARGET multicolor and FIRST selection (the primary quasar target selection criteria), all but 1015 of the $i < 19.1$ objects were selected. (The spectra of many of the last category of objects were obtained in observations that were not part of the primary survey.) The numbers are similar if one uses the BEST photometry and selection, although the completeness is not quite as high as with TARGET values.

5.1. Discrepancies Between the DR5 and Other Quasar Catalogs

The DR3 database is entirely contained in that of DR5, but there are 66 quasars from Paper III (out of 46,420 objects) that do not have a counterpart within 1.0″ of a DR5 quasar. Three of these "missing" quasars are in the DR5 list; changes in celestial position of 1.1″, 1.8″, and 5.3″ between DR3 and DR5 caused these quasars to be missed with the 1.0″ matching criterion. The other 63 cases (0.14% of the DR3 total) were individually investigated. Three DR3 objects were dropped because the latest photometry reduced their luminosities below the catalog limit. The remaining 60 objects were removed because 1) the visual examination of the spectrum either convinced us that the object was not a quasar or that the S/N was insufficient to assign a redshift with confidence or 2) The widest line in the latest fit to the spectrum had a FWHM of less than 1000 km s^{-1}. It should be noted that there have been no changes to the DR3 spectra in the DR5 database; the missing objects reflect the inherent uncertainties involved with interpreting objects that either lie near survey cutoffs or have spectra of marginal S/N.

There are 40 and 136 DR5 quasars that have redshifts that differ by more than 0.1 from the DR3 and NED values, respectively (there is, of course, considerable overlap in these two groups). In all cases the DR5 measurements are considered more reliable than those presented in previous publications. The 40 objects with $|z_{\rm DR5} - z_{\rm DR3}| > 0.1$ are listed in Table 4.

5.2. Quasar Colors

It has long been known that the majority of quasars inhabit a restricted range in photometric color, and the large sample size and accurate photometry of the SDSS revealed a relatively tight color-redshift correlation for quasars (Richards et al. 2001). This SDSS color relation, recently presented in Hopkins et al. (2004), has led to considerable success in assigning photometric redshifts to quasars (e.g., Weinstein et al. 2004 and references therein). All photometric measurements used in these analyses have been corrected for Galactic extinction.

The dependence of the four standard SDSS colors on redshift for the DR5 quasars is given in Figure 7. The dashed line in each panel is the modal relation for the DR5 quasars; the modal relations are tabulated in Table 5, along with the values for $(g - i)$. The figures show an impressively tight correlation of color with redshift, although the scatter dramatically increases when the Lyman α forest dominates the bluer of the passbands used to form the color. The distribution near the modal curve is roughly symmetric, but there is clearly a

significant population of "red" quasars that has no "blue" counterpart.

This table is an improvement over previous work in that it is based on a larger sample size (a factor of four increase since this relation was last published) and provides higher redshift resolution (0.01, except near the extrema). As in Hopkins et al. (2004), we compute the mode, rather than the mean or median, as the most representative quantity. However, a formal computation of the mode requires binning the data both in redshift and by color within redshift bins; therefore we estimated the mode from the mean and the median. Typically, the mode is estimated as (3 × median−2 × mean), but we found empirically that (2 × median−mean) appeared to work better for this sample in terms of tracing the modal "ridgeline" with redshift.

For each of the DR5 quasars we provide the quantity $\Delta(g-i)$, which is defined by

$$\Delta(g-i) \;=\; (g-i)_{\rm QSO} \;-\; \langle (g-i) \rangle_{\rm redshift}$$

where $\langle (g-i) \rangle_{\rm redshift}$ is the entry in Table 5 for the redshift of the quasar. This "differential color" provides an estimate of the continuum properties of the quasar (values above zero indicate that the object has a redder continuum than the typical quasar at that redshift).

5.3. Bright Quasars

Although the spectroscopic survey is limited to objects fainter than $i \approx 15$, the SDSS continues to discover a number of "PG-class" (Schmidt & Green 1983) objects. The DR5 catalog contains 81 entries with $i < 16.0$; 14 of the quasars are attributed to the SDSS by NED. The spectrum of the brightest post-DR3 discovery, SDSS J165551.37+214601.8 ($i = 15.62$, $z = 0.15$), is presented in Figure 1. Three of the SDSS-discovered objects in this catalog have been added since Paper III.

5.4. Luminous Quasars

There are 103 catalog quasars with $M_i < -29.0$ (3C 273 has $M_i \approx -26.6$ in our adopted cosmology); 61 were discovered by the SDSS, and 18 are published here for the first time. The redshifts of these quasars lie between 1.3 and 5.0. 2MASSI J0745217+473436 (= SDSS J074521.78+473436.
at $M_i = -30.27$ and $z = 3.22$, is the most luminous quasar in the catalog. Spectra of the two most luminous post-DR3 discoveries, with absolute i magnitudes of −29.65 and −29.94, are displayed in the upper two panels of Figure 1. The spectra of both quasars possess a

considerable number of absorption features redward of the Lyman α emission line.

5.5. Broad Absorption Line Quasars

The SDSS quasar selection algorithm has proven to be effective at finding a wide variety of Broad Absorption Line (BAL) Quasars. An EDR sample of 118 BAL quasars was presented by Tolea, Krolik, & Tsvetanov (2002). There have been two editions of the SDSS BAL Quasar Catalog; the first, associated with Paper I, contained 224 BAL quasars (Reichard et al. 2003); the second was based on the Paper III catalog and presents 4787 BAL quasars (Trump et al. 2006). BAL quasars are usually recognized by the presence of C IV absorption features, which are only visible in SDSS spectra at $z > 1.6$, thus the frequency of the BAL quasar phenomenon cannot be found from simply taking the ratio of BAL quasars to total number of quasars in the SDSS catalog. The SDSS has discovered a wide variety of extreme BAL quasars (see Hall et al. 2002); the lower right panel in Figure 1 presents the spectrum of an unusual FeLoBAL quasar with strong Balmer absorption (see Hall 2007 for a discussion of this object).

5.6. Quasars with Redshifts Below 0.15

The catalog contains 109 quasars with redshifts below 0.15. All of these objects are of low luminosity ($M_i > -24.0$, only three have $M_i < -23.5$) because of the $i \approx 15.0$ limit for the spectroscopic sample. About three-quarters of these quasars (83) are extended in the SDSS image data. A total of 40 of the $z < 0.15$ quasars were found by the SDSS; 21 have been added since Paper III.

5.7. High-Redshift ($z \geq 4$) Quasars

At first light of the SDSS, the most distant known quasar was PC 1247+3406 at redshift of 4.897 (Schneider, Schmidt, and Gunn 1991), which had been discovered seven years earlier. Within a year of operation, the SDSS had discovered quasars with redshifts above five (Fan et al. 1999, 2000); the DR5 catalog contains 60 objects with redshifts greater than that of PC 1247+3406.

In recent years the SDSS has identified quasars out to a redshift of 6.4 (Fan et al. 2003, 2006b). Quasars with redshifts larger than ≈ 5.7, however, cannot be found by the SDSS spectroscopic survey because at these redshifts the observed wavelength of the Lyman α

emission line is redward of the i band; at this point quasars become single-filter (z) detections. At the typical z-band flux levels for redshift six quasars, there are simply too many "false-positives" to undertake automated targeting. The largest redshift in the DR5 catalog is SDSS J023137.65−072854.5 at $z = 5.41$, which was originally described by Anderson et al. (2001).

The DR5 catalog contains 891 quasars with redshifts larger than four; 36 entries have redshifts above five (11 above $z = 5.2$), which is more than a factor of two increase since Paper III. The spectra of the 20 highest redshift post-DR3 objects (all with redshifts greater than or equal to 4.99) are displayed in Figure 8. These redshift five spectra display a striking variety of emission line properties, and include an impressive BAL at $z = 5.27$.

We have used archival data from *Chandra*, *ROSAT*, and *XMM-Newton* to check for new X-ray detections of $z > 4$ quasars with unusual emission-line or absorption-line properties; we do not report all $z > 4$ X-ray detections here as there are now more than 110 already published.[3] We found three remarkable $z > 4$ X-ray detections: the $z = 4.26$ BAL quasar SDSS J133529.45+410125.9, the $z = 4.11$ BAL quasar SDSS J142305.04+240507.8, and the $z = 4.50$ quasar SDSS J150730.63+553710.8, which shows remarkably strong C IV emission. None of these objects has sufficient counts for detailed X-ray spectral analysis, but we have computed their point-to-point spectral slopes between rest-frame 2500 Å and 2 keV ($\alpha_{\rm ox}$), adopting the assumptions in §2 of Brandt et al. (2002). SDSS J133529.45+410125.9 and SDSS J142305.04+240507.8 were serendipitously detected in archival *Chandra* ACIS observations and have $\alpha_{\rm ox} = -2.19$ and $\alpha_{\rm ox} = -1.52$, respectively. Comparing these values to the established relation between $\alpha_{\rm ox}$ and 2500 Å luminosity (e.g., Steffen et al. 2006), we find that SDSS J133529.45+410125.9 is notably X-ray weak, indicating likely X-ray absorption as is often seen in BAL quasars (e.g., Gallagher et al. 2006) including those at $z > 4$ (Vignali et al. 2005). In contrast, the level of X-ray emission from SDSS J142305.04+240507.8 is consistent with that from normal, non-BAL quasars; its relatively narrow UV absorption, for a BAL quasar, may indicate a relatively small column density of obscuring material. SDSS J150730.63+553710.8 is weakly detected in a *ROSAT* PSPC observation and has $\alpha_{\rm ox} = -1.47$; this level of X-ray emission is nominal for a quasar of its luminosity.

We have also checked all quasars with $z > 5$ for new X-ray detections and found none; 21 quasars with $z > 5$ have previously reported X-ray detections.

[3]See http://www.astro.psu.edu/users/niel/papers/highz-xray-detected.dat for a list of X-ray detections and references.

5.8. Close Pairs

The mechanical constraint that SDSS spectroscopic fibers must be separated by 55″ on a given plate makes it difficult for the spectroscopic survey to confirm close pairs of quasars. In regions that are covered by more than one plate, however, it is possible to obtain spectra of both components of a close pair; there are 346 pairs of quasars in the catalog with angular separation less than an arcminute (34 pairs with separations less than 20″). Most of the pairs are chance superpositions, but there are many sets whose components have similar redshifts, suggesting that the quasars may be physically associated. The typical uncertainty in the measured value of the redshift difference between two quasars is 0.02; the catalog contains 18 quasar pairs with separations of less than an arcminute and with $\Delta z < 0.02$. These pairs, which are excellent candidates for binary quasars, are listed in Table 6. Hennawi et al. (2006) identified over 200 quasar pairs in the SDSS, primarily through spectroscopic observations of SDSS quasar candidates (based on photometric measurements) near known SDSS quasars; statistical arguments based on a correlation-function analysis suggests that most of these pairs are indeed physically associated.

5.9. Morphology

The images of 3498 of the DR5 quasars are classified as extended by the SDSS photometric pipeline; 3291 (94%) have redshifts below one (there are nine resolved $z > 3.0$ quasars). The majority of the large-redshift "resolved" quasars are probably measurement errors, but this sample may also contain a mix of chance superpositions of quasars and foreground objects or possibly some small angle separation gravitational lenses (indeed, several lenses are present in the resolved quasar sample; see Paper II and Oguri et al. 2006).

5.10. Matches with Non-optical Catalogs

A total of 6226 catalog objects are FIRST sources (defined by a SDSS-FIRST positional offset of less than 2.0″). Note that 226 of the objects were selected (with TARGET) solely because they were FIRST matches (all unresolved SDSS sources brighter than $i = 19$ that lie within 2.0″ of a FIRST source are targeted by the quasar spectroscopic selection algorithm). Extended radio sources may be missed by this matching. The upper left panel in Figure 9 contains a histogram of the angular offsets between the SDSS and FIRST positions; the solid line is the expected distribution assuming a 0.21″ 1σ Gaussian error in the relative SDSS/FIRST positions (found by fitting the points with a separation less than 1.0″. The

small-angle separations are well-fit to the Rayleigh distribution, but outside of about 0.5″ there is an obvious excess of observed separations. The number of chance superpositions was estimated by shifting the quasar positions by ±200″ in declination and matching the new coordinates to the FIRST catalog; only about 0.1% of the reported FIRST matches are false. The large "tail" of this distribution is not likely to be due to measurement errors but probably arises from extended radio emission that may not be precisely centered on the optical image. To recover radio quasars that have offsets of more than 2.0″, we separately identify all objects with a greater than 3σ detection of FIRST flux at the optical position (2440 sources). For these objects as well as those with a FIRST catalog match within 2″, we perform a second FIRST catalog search with 30″ matching radius to identify possible radio lobes associated with the quasar, finding such matches for 1596 sources.

Matches with the *ROSAT* All-Sky Survey Bright and Faint Source Catalogs were made with a maximum allowed positional offset of 30″; this is the positional coincidence required for the SDSS *ROSAT* target selection code. The DR5 catalog contains 4133 RASS matches; approximately 1.3% are expected to be false identifications based on an analysis similar to that described in the previous paragraph. The SDSS-RASS offsets for the DR5 sample are presented in the upper right panel of Figure 9; the solid curve, which is the predicted distribution for a 1σ positional error of 10.34″ (fit using all the points), matches the data quite well.

JHK photometric measurements for 9824 DR5 quasars were found by using a matching radius of 2.0″ in the 2MASS All-Sky Data Release Point Source Catalog. No infrared information was used to select the SDSS spectroscopic targets. The positional offset histogram, given in the lower left panel of Figure 9, is considerably tighter than that for the FIRST matches, although the Rayleigh fit to the separations less than 1.0″ is virtually identical to the FIRST distribution (1σ of 0.21″). There are very few 2MASS identifications with offsets between 1″ and 2″; virtually all of the infrared matches are correct.

6. Summary

The lower right panel in Figure 9 charts the progress of the SDSS Quasar Survey, denoted by the number of spectroscopically-confirmed quasars, over the duration of SDSS-I. Although SDSS-I has now been completed, the SDSS Quasar Survey is continuing under the SDSS-II project. By necessity the SDSS spectroscopy lags the SDSS imaging; at the conclusion of SDSS-I more than 2000 square degrees of SDSS image data in the Northern Galactic Cap lacked spectroscopic coverage (Adelman-McCarthy et al. 2007). A future edition of the SDSS Quasar Catalog will incorporate the observations from SDSS-II and should contain

approximately 100,000 quasars.

The publication of this catalog marks the completion of the SDSS-I Quasar Survey, and we dedicate this work to the memory of John N. Bahcall. John was the initial co-chair of the SDSS Quasar Working Group, a position he held for nearly a decade. He played a key role in the formation of the SDSS Collaboration and the design of the SDSS Quasar Survey, and was a mentor to many of the members of the Quasar Working Group. We would like to thank Todd Boroson for suggesting several redshift adjustments to some of the DR3 Quasar Catalog redshifts. This work was supported in part by National Science Foundation grants AST-0307582 and AST-0607634 (DPS, DVB, JW), AST-0307384 (XF), and AST-0307409 (MAS), and by NASA LTSA grant NAG5-13035 (WNB, DPS). PBH acknowledges support by NSERC, and GTR was supported in part by a Gordon and Betty Moore Fellowship in Data Intensive Sciences at JHU. XF acknowledges support from an Alfred P. Sloan Fellowship and a David and Lucile Packard Fellowship in Science and Engineering. SJ was supported by the Max-Planck-Gesellschaft (MPI für Astronomie) through an Otto Hahn fellowship. CS was supported by the U.S. Department of Energy under contract DE-AC02-76CH03000.

Funding for the SDSS and SDSS-II has been provided by the Alfred P. Sloan Foundation, the Participating Institutions, the National Science Foundation, the U.S. Department of Energy, the National Aeronautics and Space Administration, the Japanese Monbukagakusho, the Max Planck Society, and the Higher Education Funding Council for England. The SDSS Web site is `http://www.sdss.org/`.

The SDSS is managed by the Astrophysical Research Consortium (ARC) for the Participating Institutions. The Participating Institutions are the American Museum of Natural History, Astrophysical Institute of Potsdam, University of Basel, Cambridge University, Case Western Reserve University, University of Chicago, Drexel University, Fermilab, the Institute for Advanced Study, the Japan Participation Group, Johns Hopkins University, the Joint Institute for Nuclear Astrophysics, the Kavli Institute for Particle Astrophysics and Cosmology, the Korean Scientist Group, the Chinese Academy of Sciences (LAMOST), Los Alamos National Laboratory, the Max-Planck-Institute for Astronomy (MPIA), the Max-Planck-Institute for Astrophysics (MPA), New Mexico State University, Ohio State University, University of Pittsburgh, University of Portsmouth, Princeton University, the United States Naval Observatory, and the University of Washington.

This research has made use of 1) the NASA/IPAC Extragalactic Database (NED) which is operated by the Jet Propulsion Laboratory, California Institute of Technology, under contract with the National Aeronautics and Space Administration, and 2) data products from

the Two Micron All Sky Survey, which is a joint project of the University of Massachusetts and the Infrared Processing and Analysis Center/California Institute of Technology, funded by the National Aeronautics and Space Administration and the National Science Foundation.

REFERENCES

Abazajian, K., et al. 2003, AJ, 126, 2081 (DR1)

Abazajian, K., et al. 2005, AJ, 129, 1755 (DR3)

Adelman-McCarthy, J., et al. 2006, ApJS, 162, 38 (DR4)

Adelman-McCarthy, J., et al. 2007, ApJS, in press (DR5)

Anderson, S.F., et al. 2001, AJ, 122, 503

Anderson, S.F., et al. 2003, AJ, 126, 2209

Anderson, S.F., et al. 2007, AJ, 133, 313

Becker, R.H., White, R.L., & Helfand, D.J. 1995, ApJ, 450, 559

Bell, M. B., & McDiarmid, D. 2006, ApJ, 648, 140

Blanton, M.R., Lupton, R.H., Maley, F.M., Young, N., Zehavi, I., & Loveday, J. 2003, AJ, 125, 2276

Brandt, W.N., et al. 2002, ApJ, 569, L5

Castander, F.J., et al. 2001, AJ, 121, 2331

Collinge, M., et al. 2005, AJ, 129, 2542; Erratum AJ 131, 3135

Cutri, R.M., Skrutskie, M.F., van Dyk, S., Beichman, C.A., et al. 2003, VizieR On-line Data Catalog: II/246, University of Massachusetts and Infrared Processing and Analysis Center

Eisenstein, D.J., et al. 2001, AJ, 122, 2267

Elvis M., Lockman F.J., & Fassnacht C., 1994, ApJS, 95, 413

Fan, X., et al. 1999, AJ, 118, 1

Fan, X., et al. 2000, AJ, 119, 1

Fan, X., et al. 2003, AJ, 125, 1649

Fan, X., et al. 2006a, AJ, 131, 1203

Fan, X., et al. 2006b, AJ, 132, 171

Fukugita, M., Ichikawa, T., Gunn, J.E., Doi, M., Shimasaku, K., & Schneider, D.P. 1996, AJ, 111, 1748

Gallagher, S.C., Brandt, W.N., Chartas, G., Priddey, R., Garmire, G.P., & Sambruna, R.M. 2006, ApJ, 644, 709

Gaskell, C.M. 1982, ApJ, 263, 79

Gunn, J.E., et al. 1998, AJ, 116, 3040

Gunn, J.E., et al. 2006, AJ, 131, 2332

Hall, P.B. 2007, AJ, 133, 1271

Hall, P.B., et al. 2002, ApJS, 141, 267

Hennawi, J., et al. 2006, 131, 1

Hao, L., et al. 2005, AJ, 129, 1783

Hogg, D.W., Schlegel, D.J., Finkbeiner, D.P., & Gunn, J.E. 2001, AJ, 122, 2129

Hopkins, P.F., et al. 2004, AJ, 128, 1112

Ivezić, Ž., et al. 2002, AJ, 124, 2364

Ivezić, Ž., et al. 2004, AN, 325, 583

Kauffmann, G., et al. 2003, MNRAS, 346, 1055

Lupton, R.H., Gunn, J.E., Ivezić, Ž., Knapp, G.R., Kent, S., & Yasuda, N. 2001, in ASP Conf. Ser. 238, Astronomical Data Analysis Software and Systems, ed. F.R. Harnden, F.A. Primini, & H.E. Payne (San Francisco:ASP), 269

Lupton, R.H., Gunn, J.E., & Szalay, A. 1999, AJ, 118, 1406

Oke, J.B., & Gunn, J.E., 1983, ApJ., 266, 713 Oguri, M., et al. 2006, AJ, 132, 999

Pier, J.R., Munn, J.A., Hindsley, R.B., Hennessy, G.S., Kent, S.M., Lupton, R.H., & Ivezić, Ž., 2003, AJ, 125, 1559

Reichard, T.A., et al. 2003, AJ, 125, 1711

Richards, G.T., et al. 2001, AJ, 121, 2308

Richards, G.T., et al. 2002a, AJ, 123, 2945

Richards, G.T., et al. 2002b, AJ, 124,1

Richards, G.T., et al. 2006, AJ, 131, 2766

Schlegel, D.J., Finkbeiner, D.P., & Davis, M. 1998, ApJ, 500, 525

Schmidt, M., & Green, R.F. 1983, ApJ, 269, 352

Schneider, D.P., Gunn, J.E., & Hoessel, J.G. 1983, ApJ, 264, 337

Schneider, D.P., Schmidt, M., and Gunn, J.E., 1991, AJ, 102, 837

Schneider, D.P., et al. 2002, AJ, 123, 567 (Paper I)

Schneider, D.P., et al. 2003, AJ, 126, 2579 (Paper II)

Schneider, D.P., et al. 2005, AJ, 130, 367 (Paper III)

Shen, Y., et al. 2007, AJ, in press.

Skrutskie, M.F., et al. 2006, AJ, 131, 1163

Smith, J.A., et al. 2002, AJ, 123, 2121

Spergel, D.N., et al. 2006, ApJ, submitted (astro-ph/0603449)

Stark A.A., Gammie C.F., Wilson R.W., Bally J., Linke R.A., Heiles, C., & Hurwitz, M. 1992, ApJS, 79, 77

Steffen, A.T., Strateva, I.V., Brandt, W.N., Alexander, D.M., Koekemoer, A.M., Lehmer, B.D., Schneider, D.P., & Vignali, C. 2006, AJ, 131, 2826

Stoughton, C., et al. 2002, AJ, 123, 485 (EDR)

Strauss, M.A., et al. 2002, AJ, 124, 1810

Tolea, A., Krolik, J.H., & Tsvetanov, Z. 2002, ApJ, 578, 31

Trump, J.R., et al. 2006, ApJS, 165, 1

Tucker, D., et al. 2006, AN, 327, 821

Vanden Berk, D.E., et al. 2001, AJ, 122, 549

Vanden Berk, D.E., et al. 2005, AJ, 129, 2047

Vignali, C., Brandt, W.N., Schneider, D.P., & Kaspi, S. 2005, AJ, 129, 2519

Voges, W., et al. 1999, A & A, 349, 389

Voges, W., et al. 2000, IAUC, 7432

Weinstein, M.A., et al. 2004, ApJS, 155, 243

Wilhite, B.C., et al. 2005, AJ, 633, 638

York, D.G., et al. 2000, AJ, 120, 1579

Zacharias, N., et al. 2000, AJ, 120, 2131

Zakamska, N.L., et al. 2003, AJ, 128, 1002

This preprint was prepared with the AAS LaTeX macros v5.2.

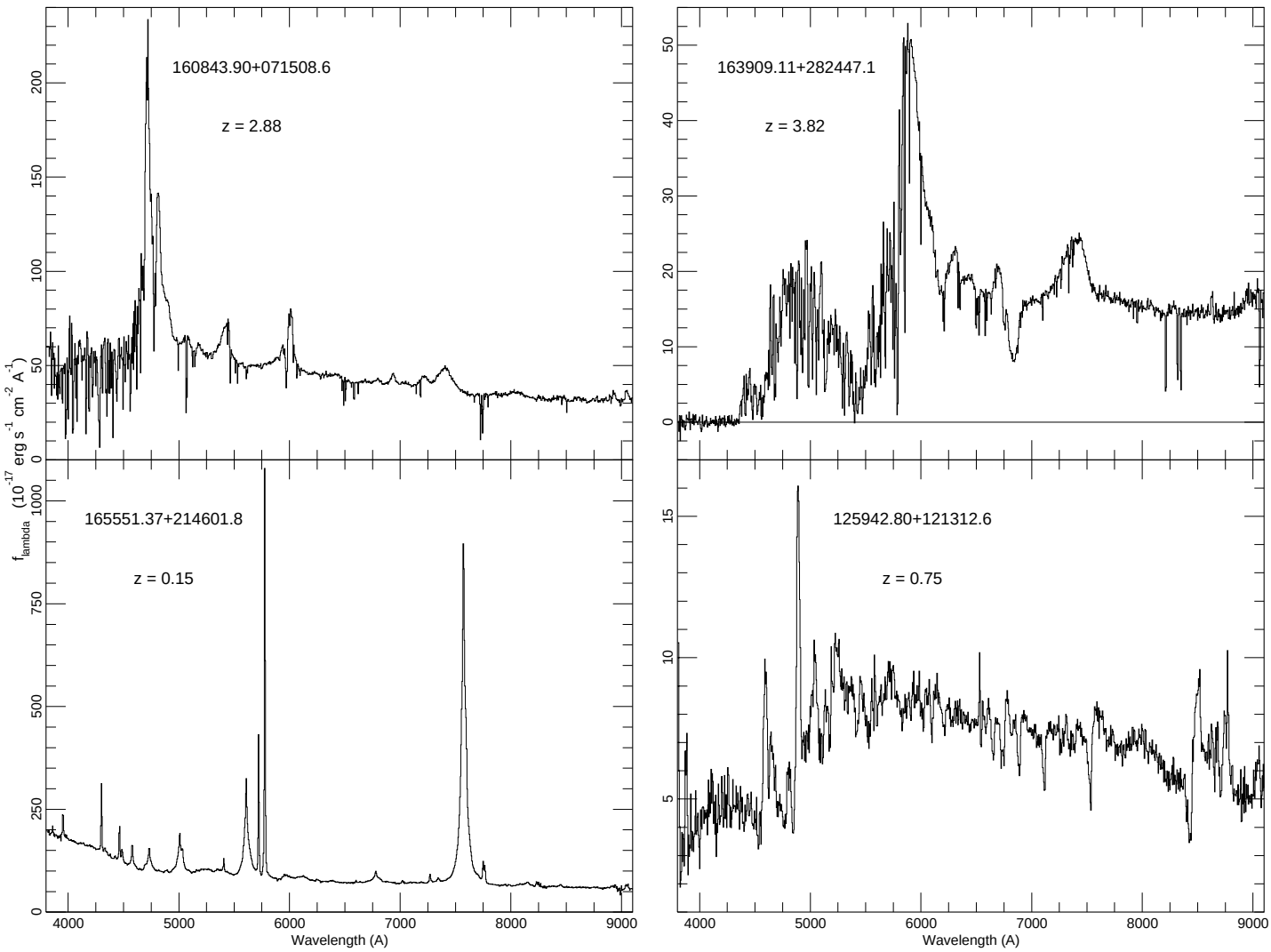

Fig. 1.— SDSS spectra of four previously unreported quasars. The spectral resolution of the data ranges from 1800 to 2100; a dichroic splits the beam at 6150 Å. The data have been rebinned to 5 Å pixel^{-1} for display purposes. The upper two panels display the two most luminous of the newly discovered quasars; both objects have $M_i < -29.6$. SDSS J165551.37+214601.8 is the brightest ($i = 15.62$) of the new quasars; SDSS J125942.80+121312.6 is an unusual FeLoBAL quasar with Balmer-line absorption.

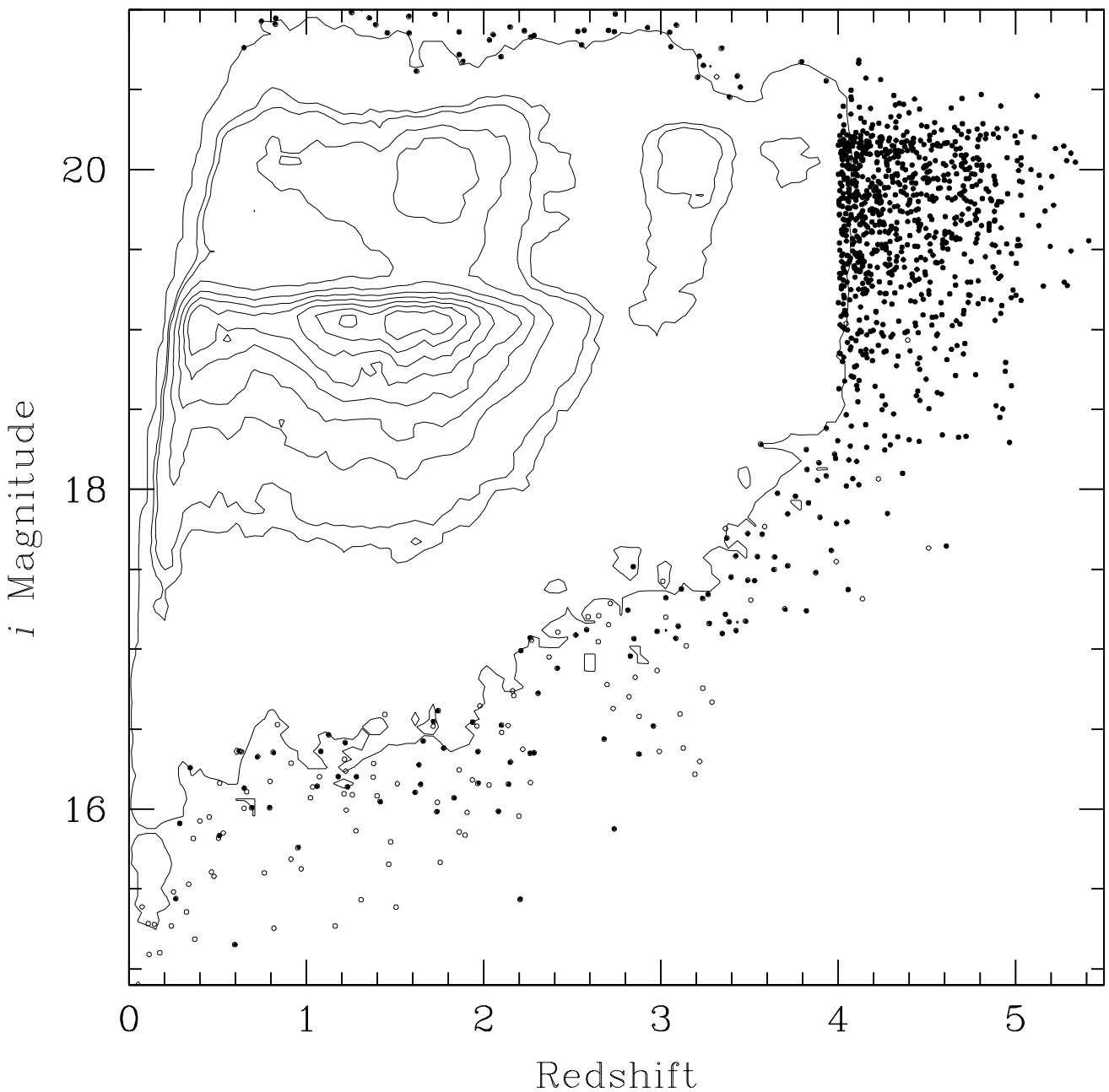

Fig. 2.— The observed i magnitude as a function of redshift for the 77,429 objects in the catalog. Open circles indicate quasars in NED that were recovered but not discovered by the SDSS. The 26 quasars with $i > 21$ are not plotted. The distribution is represented by a set of linear contours when the density of points in this two-dimensional space causes the points to overlap. The steep gradient at $i \approx 19$ is due to the flux limit for the targeted low-redshift part of the survey; the dip in the counts at $z \approx 2.7$ arises because of the high incompleteness of the SDSS Quasar Survey at redshifts between 2.5 and 3.0 (also see Figure 3).

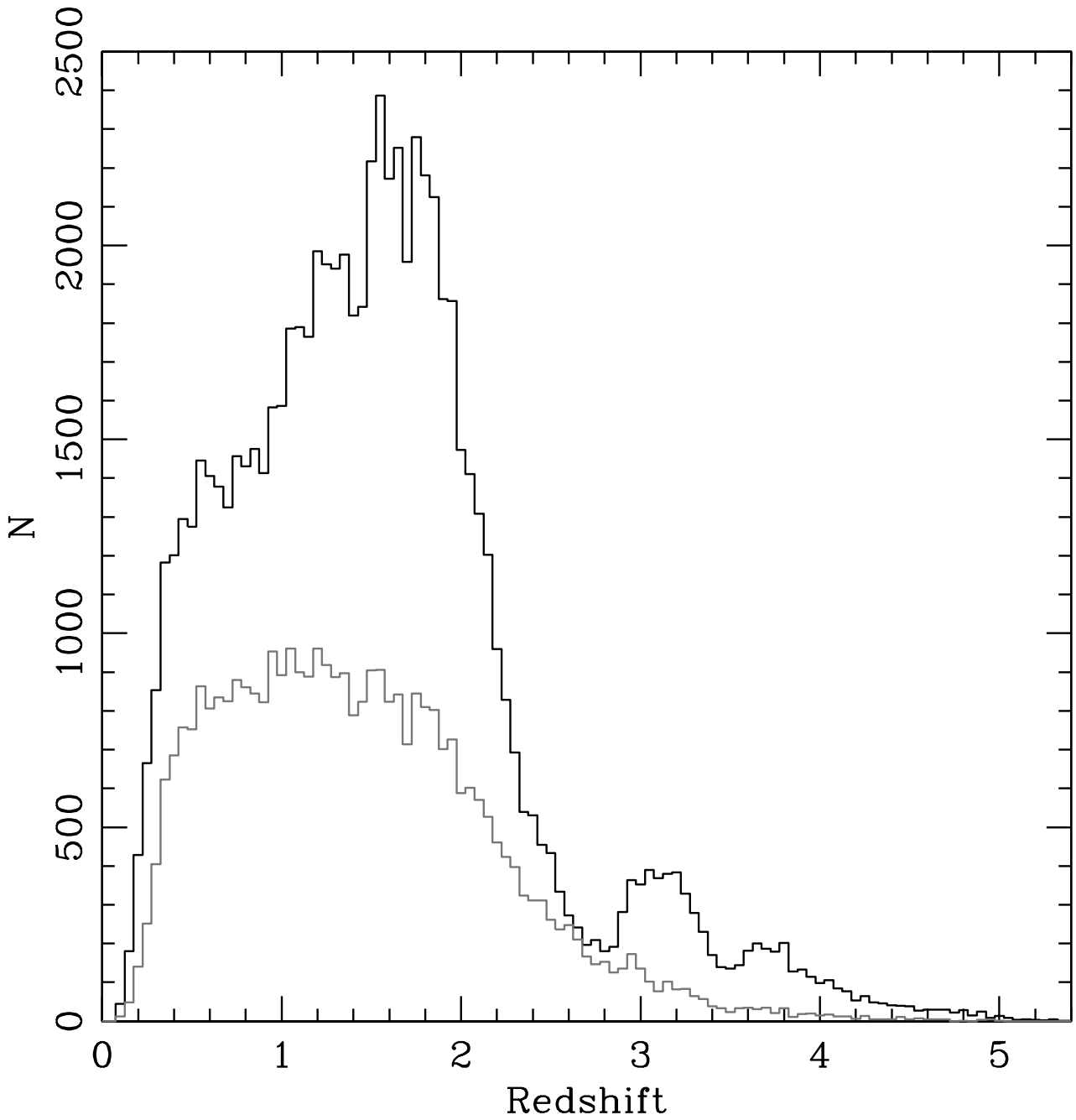

Fig. 3.— The redshift histogram of the catalog quasars. The redshifts range from 0.08 to 5.41; the median redshift of the catalog is 1.48. The redshift bins have a width of 0.05. The dips at redshifts of 2.7 and 3.5 are caused by the reduced efficiency of the selection algorithm at these redshifts. The lower histogram is the redshift distribution of the $i < 19.1$ sample after correction for selection effects (see Section 5).

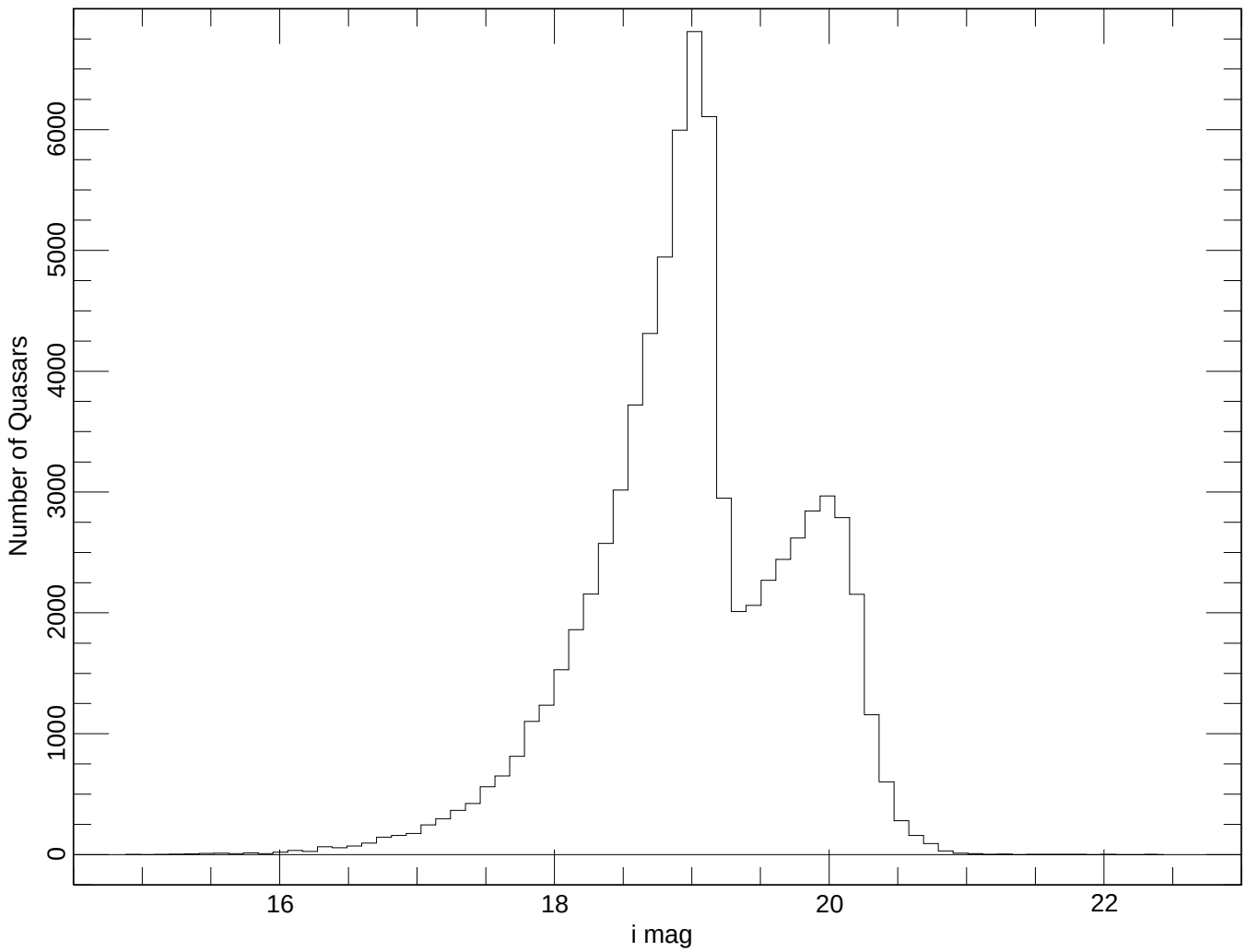

Fig. 4.— The i magnitude (not corrected for Galactic absorption) histogram of the 77,429 catalog quasars. The magnitude bins have a width of 0.108. The sharp drop that occurs at magnitudes slightly fainter than 19 is due to the flux limit for the low-redshift targeted part of the survey. Quasars fainter than the $i = 20.2$ high-redshift selection limit were found via other selection algorithms, primarily serendipity. The SDSS Quasar survey has a bright limit of $i \approx 15.0$ imposed by the need to avoid saturation in the spectroscopic observations.

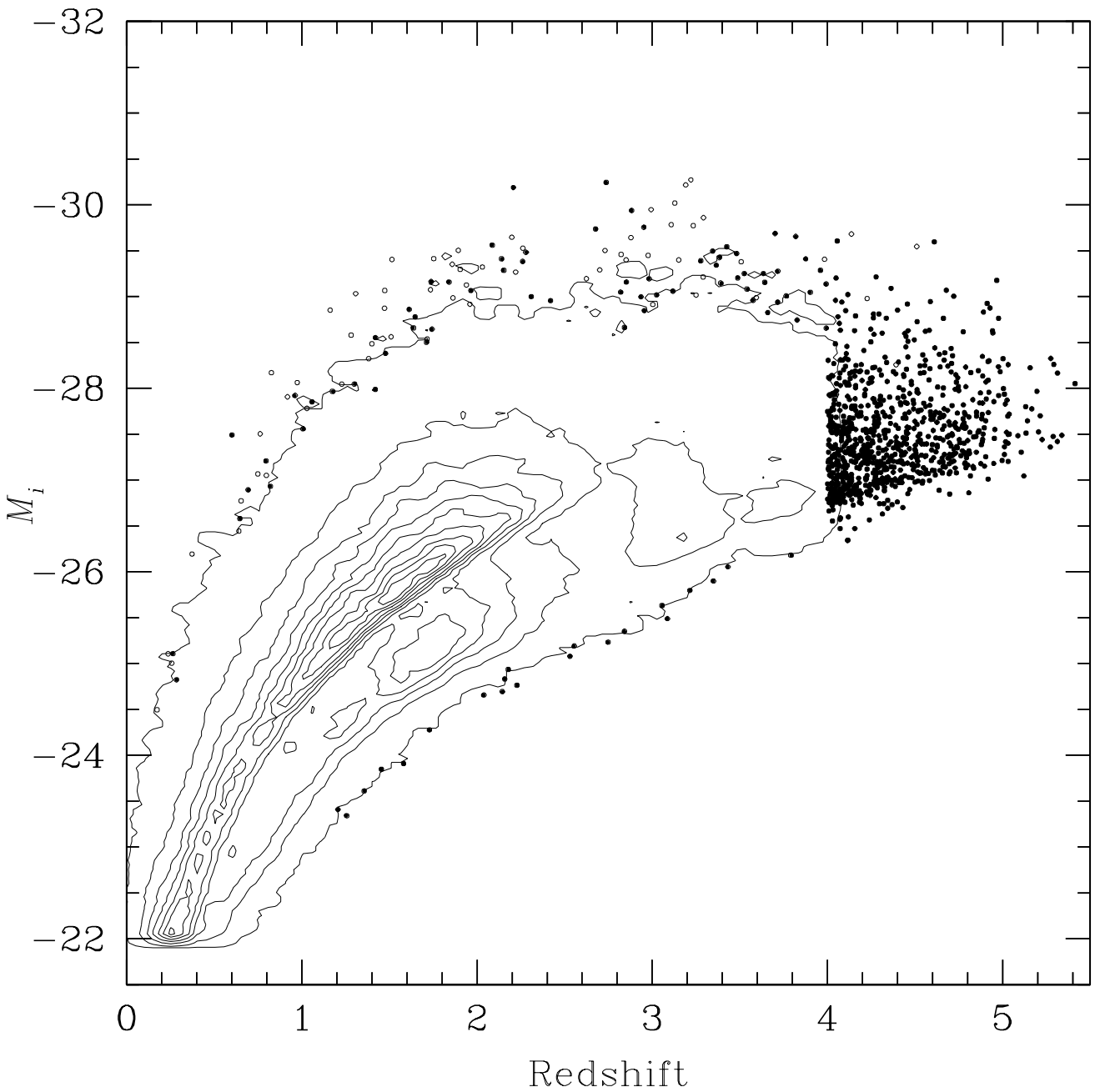

Fig. 5.— The absolute i magnitude as a function of redshift for the 77,429 objects in the catalog. Open circles indicate quasars in NED that were recovered but not discovered by the SDSS. The distribution is represented by a set of linear contours when the density of points in this two-dimensional space causes the points to overlap. The steep gradient that runs through the midst of the quasar distribution is produced by the $i \approx 19$ flux limit for the targeted low-redshift part of the survey.

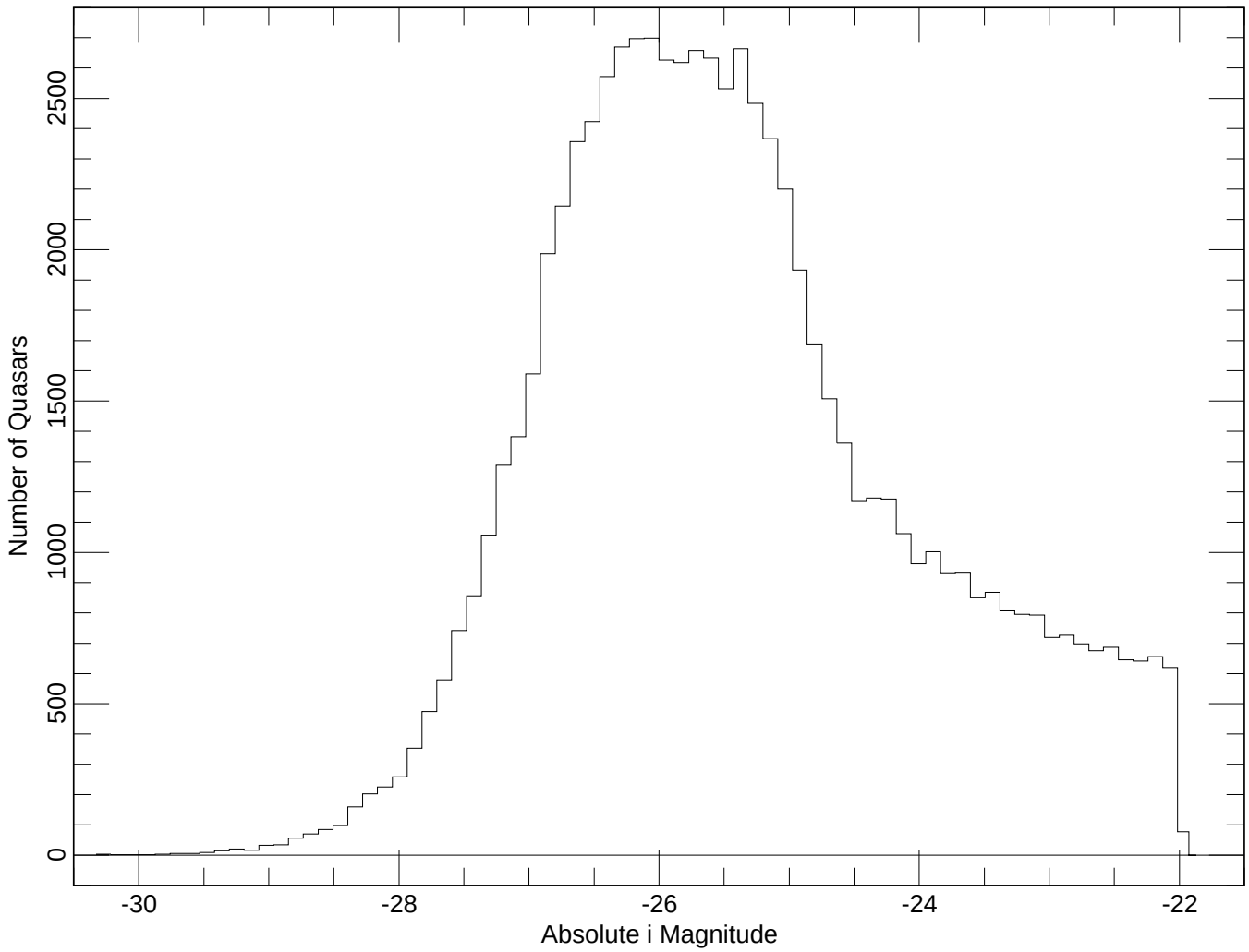

Fig. 6.— The luminosity distribution of the catalog quasars. The absolute magnitude bins have a width of 0.114. The most luminous quasar in the catalog has $M_i \approx -30.3$. In the adopted cosmology 3C 273 has $M_i \approx -26.6$.

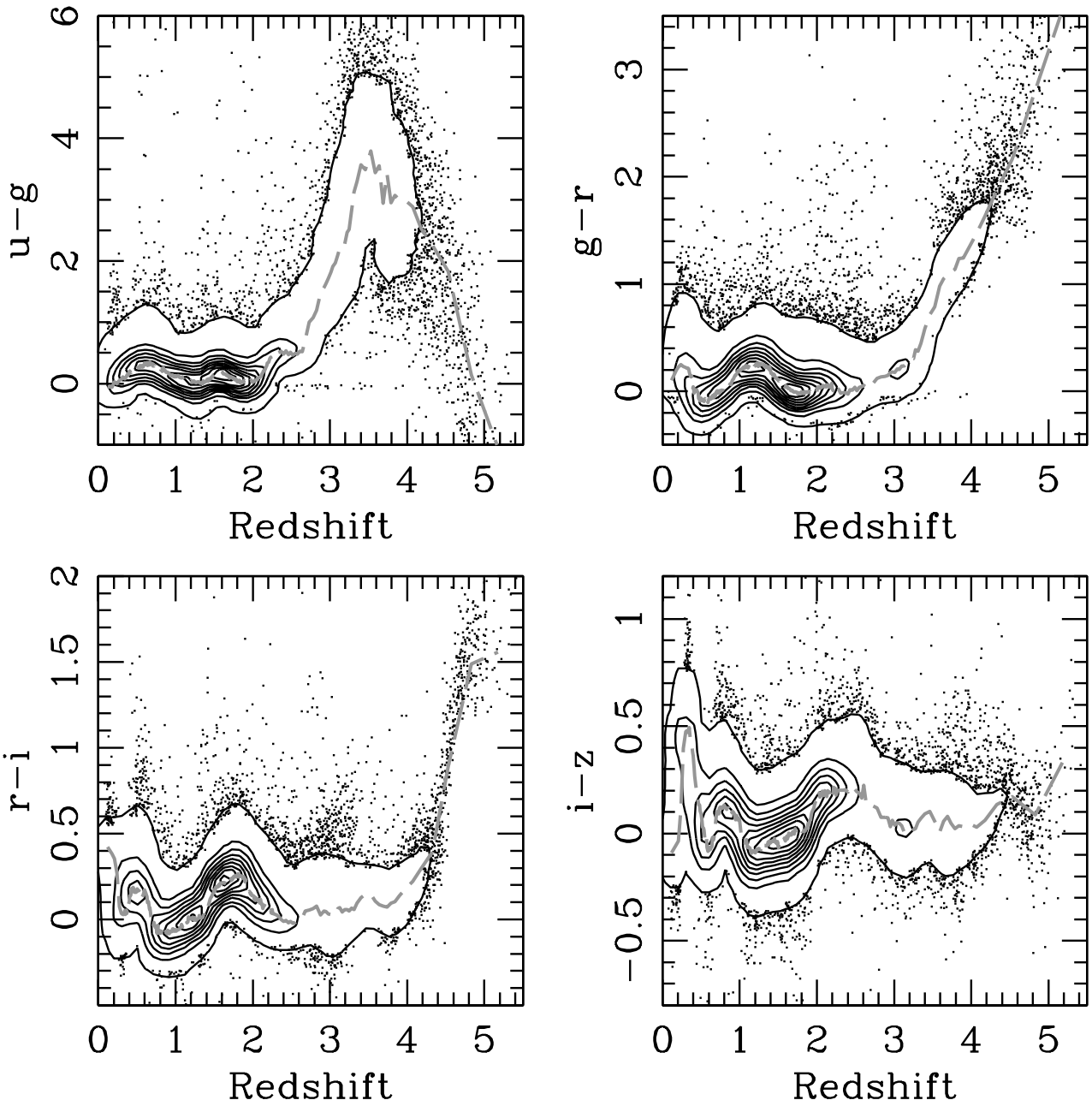

Fig. 7.— The quasar color-redshift relation for the DR5 quasars (photometry corrected for Galactic extinction). Contours are used to represent the distribution when the density of points causes the points to overlap. The panels present the four standard SDSS colors; the dashed gray lines are the modal relations presented in Table 5. The influence of emission lines on the colors is readily apparent (in particular Hα in the $(i-z)$ panel). The tightness of the correlations breaks down when the Lyman α forest region dominates the bluer of the two passbands (e.g., above redshifts of 2.2 in the $(u-g)$ relation).

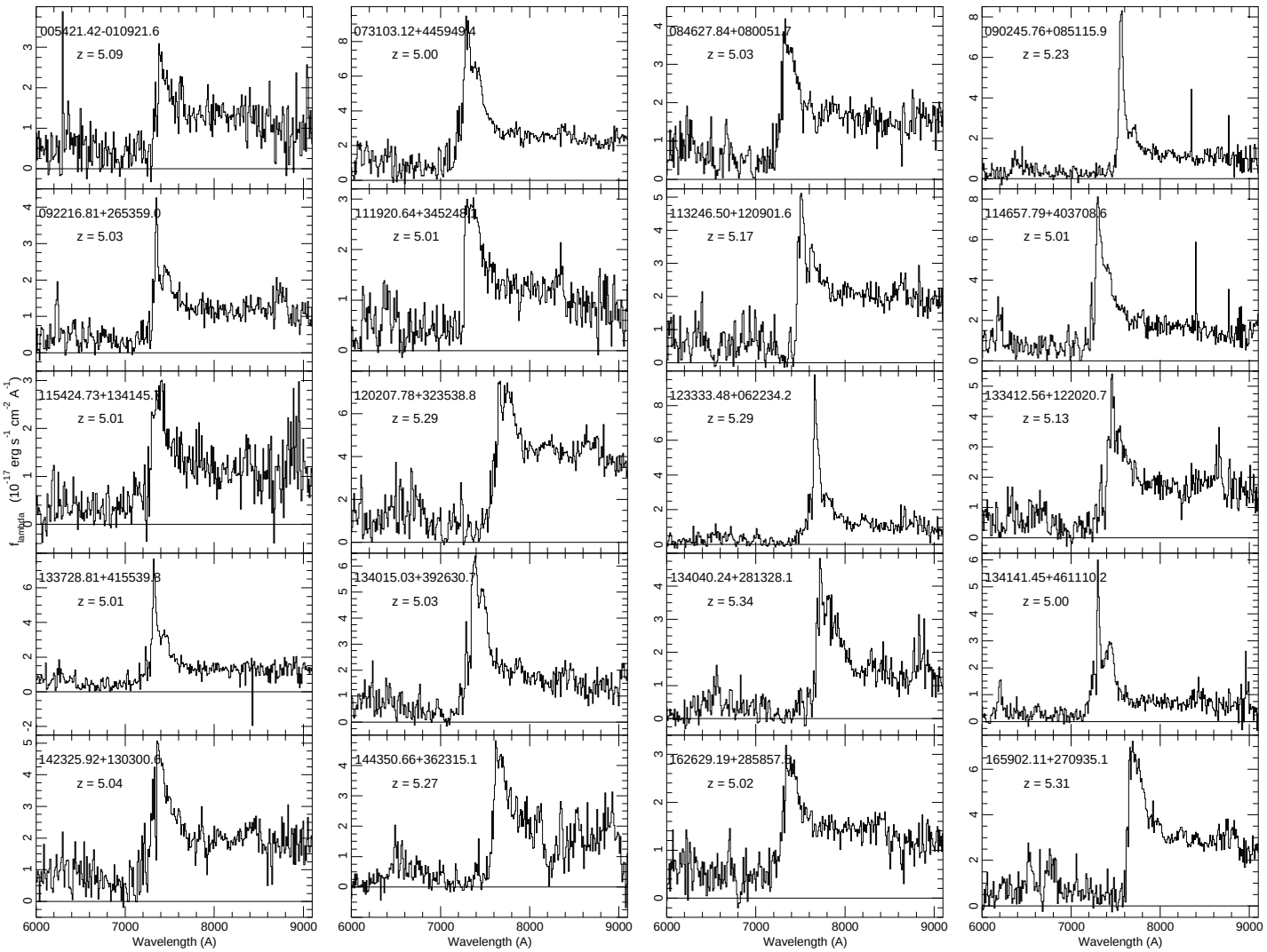

Fig. 8.— SDSS spectra of the 20 new quasars with the highest redshifts ($z \geq 4.99$). The spectra have been rebinned to 10 Å pixel^{-1} for display purposes. The wavelength region below 6000 Å has been removed because of the lack of signal below rest frame wavelengths of 1000 Å in these objects. Five of the quasars have redshifts larger than 5.25.

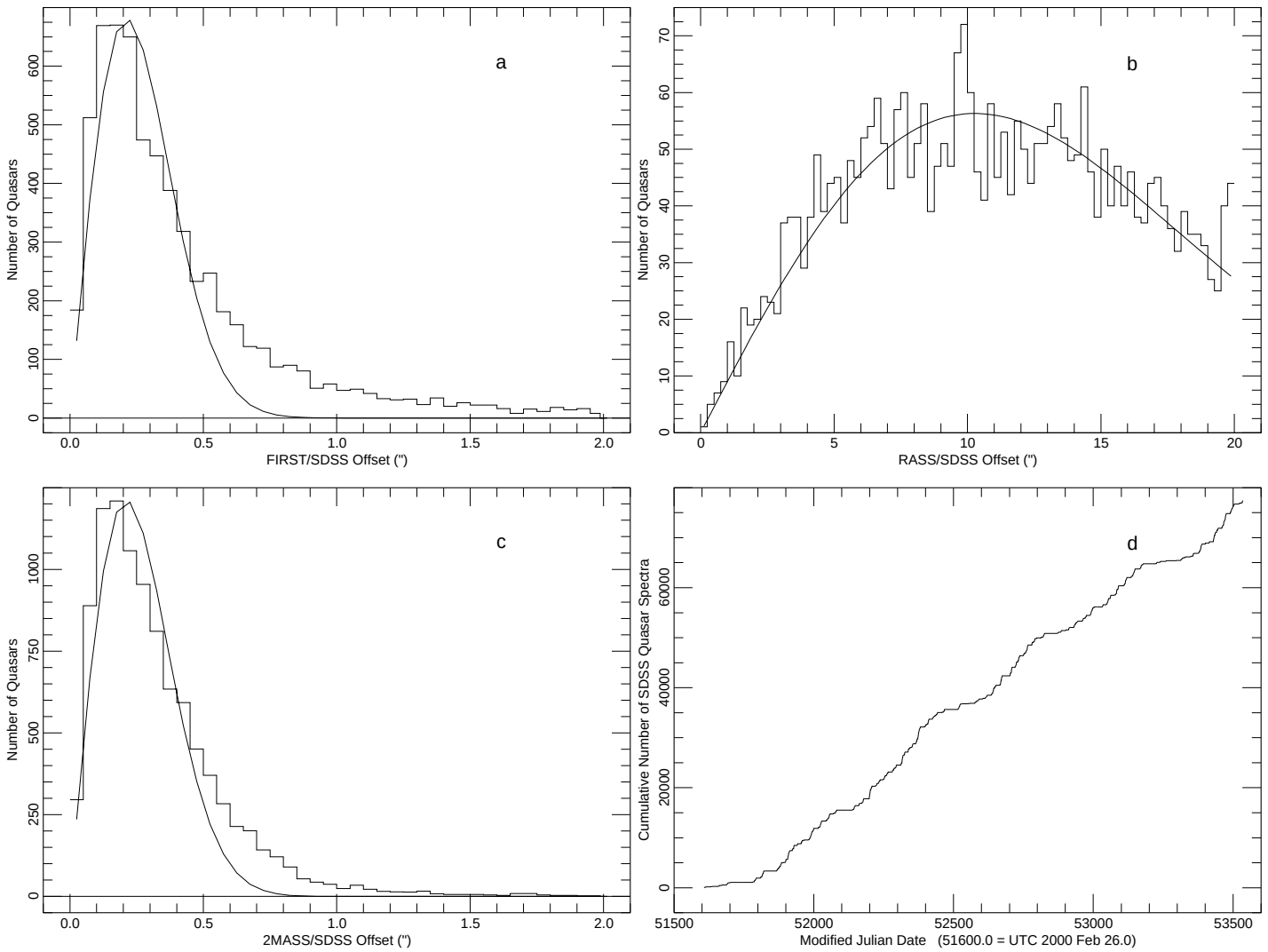

Fig. 9.— a) Offsets between the 6226 SDSS and FIRST matches; the matching radius was set to 2.0″. The smooth curve is the expected distribution for a set of matches if the offsets between the objects are described by a Rayleigh distribution with $\sigma = 0.21''$ (best fit for points with separations of less than 1.0″). b) Offsets between the 4133 SDSS and RASS FSC/BSC matches; the matching radius was set to 30″. The smooth curve is a fit to the distribution with a Rayleigh distribution with $\sigma = 10.3''$. c) Offsets between the 9824 SDSS and 2MASS matches; the matching radius was set to 2″. The smooth curve is a Rayleigh distribution with $\sigma = 0.21''$ based on the points with separations smaller than 1.0″. d) The cumulative number of DR5 quasars as a function of time. The horizontal axis runs from February 2000 to June 2005. The rougly periodic structure in the curve is caused by the yearly summer maintence schedule. The total number of objects in the catalog is 77,429.

Table 1. SDSS DR5 Quasar Catalog Format

Column	Format	Description
1	A18	SDSS DR5 Designation hhmmss.ss+ddmmss.s (J2000)
2	F11.6	Right Ascension in decimal degrees (J2000)
3	F11.6	Declination in decimal degrees (J2000)
4	F7.4	Redshift
5	F7.3	BEST PSF u magnitude (not corrected for Galactic extinction)
6	F6.3	Error in BEST PSF u magnitude
7	F7.3	BEST PSF g magnitude (not corrected for Galactic extinction)
8	F6.3	Error in BEST PSF g magnitude
9	F7.3	BEST PSF r magnitude (not corrected for Galactic extinction)
10	F6.3	Error in BEST PSF r magnitude
11	F7.3	BEST PSF i magnitude (not corrected for Galactic extinction)
12	F6.3	Error in BEST PSF i magnitude
13	F7.3	BEST PSF z magnitude (not corrected for Galactic extinction)
14	F6.3	Error in BEST PSF z magnitude
15	F7.3	Galactic extinction in u band
16	F7.3	$\log N_H$ (logarithm of Galactic H I column density)
17	F7.3	FIRST peak flux density at 20 cm expressed as AB magnitude; 0.0 is no detection, -1.0 source is not in FIRST area
18	F8.3	S/N of FIRST flux density
19	F7.3	SDSS-FIRST separation in arc seconds
20	I3	$> 3\sigma$ FIRST flux at optical position but no FIRST counterpart within $2''$ (0 or 1)
21	I3	FIRST source located $2''$-$30''$ from optical position (0 or 1)
22	F8.3	log RASS full band count rate; -9.0 is no detection
23	F7.3	S/N of RASS count rate
24	F7.3	SDSS-RASS separation in arc seconds
25	F7.3	J magnitude (2MASS); 0.0 indicates no 2MASS detection
26	F6.3	Error in J magnitude (2MASS)
27	F7.3	H magnitude (2MASS); 0.0 indicates no 2MASS detection
28	F6.3	Error in H magnitude (2MASS)
29	F7.3	K magnitude (2MASS); 0.0 indicates no 2MASS detection
30	F6.3	Error in K magnitude (2MASS)
31	F7.3	SDSS-2MASS separation in arc seconds
32	F8.3	M_i ($H_0 = 70$ km s^{-1} Mpc^{-1}, $\Omega_M = 0.3$, $\Omega_\Lambda = 0.7$, $\alpha_\nu = -0.5$)

Table 1—Continued

Column	Format	Description
33	F7.3	$\Delta(g-i) = (g-i) - \langle(g-i)\rangle_{\rm redshift}$ (Galactic extinction corrected)
34	I3	Morphology flag 0 = point source 1 = extended
35	I3	SDSS SCIENCEPRIMARY flag (0 or 1)
36	I3	SDSS MODE flag (blends, overlapping scans; 1, 2, or 3)
37	I3	Selected with final quasar algorithm (0 or 1)
38	I12	Target Selection Flag (BEST)
39	I3	Low-z Quasar selection flag (0 or 1)
40	I3	High-z Quasar selection flag (0 or 1)
41	I3	FIRST selection flag (0 or 1)
42	I3	*ROSAT* selection flag (0 or 1)
43	I3	Serendipity selection flag (0 or 1)
44	I3	Star selection flag (0 or 1)
45	I3	Galaxy selection flag (0 or 1)
46	I6	SDSS Imaging Run Number of photometric measurements
47	I6	Modified Julian Date of imaging observation
48	I6	Modified Julian Date of spectroscopic observation
49	I5	Spectroscopic Plate Number
50	I5	Spectroscopic Fiber Number
51	I4	SDSS Photometric Processing Rerun Number
52	I3	SDSS Camera Column Number
53	I5	SDSS Field Number
54	I5	SDSS Object Number
55	I12	Target Selection Flag (TARGET)
56	I3	Low-z Quasar selection flag (0 or 1)
57	I3	High-z Quasar selection flag (0 or 1)
58	I3	FIRST selection flag (0 or 1)
59	I3	*ROSAT* selection flag (0 or 1)
60	I3	Serendipity selection flag (0 or 1)
61	I3	Star selection flag (0 or 1)
62	I3	Galaxy selection flag (0 or 1)
63	F7.3	TARGET PSF u magnitude (not corrected for Galactic extinction)
64	F6.3	TARGET Error in PSF u magnitude
65	F7.3	TARGET PSF g magnitude (not corrected for Galactic extinction)

Table 1—Continued

Column	Format	Description
66	F6.3	TARGET Error in PSF g magnitude
67	F7.3	TARGET PSF r magnitude (not corrected for Galactic extinction)
68	F6.3	TARGET Error in PSF r magnitude
69	F7.3	TARGET PSF i magnitude (not corrected for Galactic extinction)
70	F6.3	TARGET Error in PSF i magnitude
71	F7.3	TARGET PSF z magnitude (not corrected for Galactic extinction)
72	F6.3	TARGET Error in PSF z magnitude
73	I21	Spectroscopic Identification flag (64-bit integer)
74	1X, A25	Object Name for previously known quasars "SDSS" designates previously published SDSS object

Table 2. The SDSS Quasar Catalog IV[a]

Object (SDSS J)	R.A. (deg)	Dec (deg)	Redshift	u		g		r		i		z		A_u
000006.53+003055.2	0.027228	0.515349	1.8227	20.389	0.066	20.468	0.034	20.332	0.037	20.099	0.041	20.053	0.121	
000008.13+001634.6	0.033898	0.276304	1.8365	20.233	0.054	20.200	0.024	19.945	0.032	19.491	0.032	19.191	0.068	
000009.26+151754.5	0.038605	15.298476	1.1986	19.921	0.042	19.811	0.036	19.386	0.017	19.165	0.023	19.323	0.069	
000009.38+135618.4	0.039088	13.938447	2.2400	19.218	0.026	18.893	0.022	18.445	0.018	18.331	0.024	18.110	0.033	
000009.42−102751.9	0.039269	−10.464428	1.8442	19.249	0.036	19.029	0.027	18.980	0.021	18.791	0.018	18.751	0.047	

[a]Table 2 is presented in its entirety in the electronic edition of the Astronomical Journal. A portion is shown here for guidance regarding its form and content. The full catalog contains 74 columns of information on 77,429 quasars.

Table 3. Spectroscopic Target Selection

Class	TARGET Selected	TARGET Sole Selection	BEST Selected	BEST Sole Selection
Low-z	49010	16422	46460	14444
High-z	16383	5327	16757	4411
FIRST	3501	226	3619	209
ROSAT	4817	380	4918	492
Serendipity	42109	15729	41042	15950
Star	1970	187	820	162
Galaxy	536	99	601	80

Table 4. Quasars with $|z_{\rm DR5} - z_{\rm DR3}| > 0.1$

SDSS J	$z_{\rm DR5}$	SDSS J	$z_{\rm DR5}$
005508.55−105206.2	1.381	133028.12+600811.7	1.992
013413.55+142900.1	1.195	133951.94+481651.3	0.911
031712.23−075850.3	2.696	134048.37+433359.8	2.069
075052.59+300334.1	3.990	135833.05+634122.6	3.180
075132.75+350535.0	2.077	140012.65+595823.3	2.061
083503.79+322242.0	0.728	140223.63+463604.9	0.925
085339.64+372203.6	1.950	140327.91+613654.2	2.023
090902.73+355334.8	1.638	141230.28+471103.7	2.078
091025.25+365921.3	2.004	142010.28+604722.3	1.345
092415.87+424632.2	0.559	143702.47+613437.0	2.064
093557.85+005528.1	1.301	144939.30+534212.1	1.805
093935.08−000801.1	0.909	151307.26−000559.3	2.030
094326.48+460226.8	2.093	151422.99+481936.3	2.071
100415.17+415802.6	1.977	153257.67+422047.1	1.950
102117.71+623010.1	1.949	160320.97+315248.3	0.727
103039.95+510923.3	1.649	165806.76+611858.9	2.631
103219.66+563456.8	2.017	170929.58+323826.9	1.902
115917.62+100921.5	2.028	205058.45+004709.9	0.932
124345.10+492645.3	1.982	212744.12+005720.3	4.386
131810.57+585416.9	1.900	225246.43+142525.8	4.904

Table 5. Quasar Colors as a Function of Redshift[a]

$z_{\rm bin}$	$\langle z \rangle$	$N_{\rm QSO}$	$(g-i)$	$(u-g)$	$(g-r)$	$(r-i)$	$(i-z)$
0.18	0.181	183	0.567	−0.065	0.197	0.379	−0.037
0.21	0.210	290	0.580	0.032	0.223	0.355	−0.034
0.24	0.240	394	0.513	0.000	0.236	0.267	0.115
0.27	0.270	406	0.289	0.055	0.231	0.077	0.397
0.30	0.301	484	0.236	0.067	0.219	0.033	0.472

[a]Table 5 is presented in its entirety in the electronic edition of the Astronomical Journal. A portion is shown here for guidance regarding its form and content.

Table 6. Candidate Binary Quasars

Quasar 1	Quasar 2	z_1	z_2	$\Delta\theta$ ″
001201.87+005259.7	001202.35+005314.0	1.652	1.642	16.0
011757.99+002104.1	011758.83+002021.4	0.612	0.613	44.5
014110.40+003107.1	014111.62+003145.9	1.879	1.882	42.9
024511.93−011317.5	024512.12−011313.9	2.463	2.460	4.5
025813.65−000326.4	025815.54−000334.2	1.316	1.321	29.4
025959.68+004813.6	030000.57+004828.0	0.892	0.900	19.6
074336.85+205512.0	074337.28+205437.1	1.570	1.565	35.5
074759.02+431805.4	074759.66+431811.5	0.501	0.501	9.2
082439.83+235720.3	082440.61+235709.9	0.536	0.536	14.9
085625.63+511137.0	085626.71+511117.8	0.543	0.543	21.8
090923.12+000203.9	090924.01+000211.0	1.884	1.865	15.0
095556.37+061642.4	095559.02+061701.8	1.278	1.273	44.0
110357.71+031808.2	110401.48+031817.5	1.941	1.923	57.3
111610.68+411814.4	111611.73+411821.5	2.980	2.971	13.8
113457.73+084935.2	113459.37+084923.2	1.533	1.525	27.1
121840.47+501543.4	121841.00+501535.8	1.457	1.455	9.1
165501.31+260517.5	165502.02+260516.5	1.881	1.892	9.6
215727.26+001558.4	215728.35+001545.5	2.540	2.553	20.8

[a]The quasar pairs were selected by a redshift difference of less than 0.02 and an angular separation less than 60″.